## Geological Magazine

#### www.cambridge.org/geo

# **Original Article**

Cite this article: Usman M, Clift P, Garzanti E, Pastore G, Vezzoli G, Munawar MJ, and Ali M. Controls on sediment supply to the Holocene Thar Desert: Sr and Nd isotopes with bulk-sediment geochemical constraints. *Geological Magazine* 162(e46): 1–18. https://doi.org/10.1017/S0016756825100320

Received: 16 June 2025 Revised: 1 October 2025 Accepted: 2 October 2025

#### Keywords:

Sand provenance; geochemistry; Sr and Nd isotopes; SW summer monsoon; Thar Desert

#### Corresponding author:

Muhammad Usman; Emails: m.usman1@campus.unimib.it, usman.pu@outlook.com

© The Author(s), 2025. Published by Cambridge University Press. This is an Open Access article, distributed under the terms of the Creative Commons Attribution licence (https://creativecommons.org/licenses/by/4.0/), which permits unrestricted re-use, distribution and reproduction, provided the original article is properly cited.



# Controls on sediment supply to the Holocene Thar Desert: Sr and Nd isotopes with bulksediment geochemical constraints

Muhammad Usman<sup>1</sup>, Peter Clift<sup>2,3</sup>, Eduardo Garzanti<sup>1</sup>, Guido Pastore<sup>1</sup>, Giovanni Vezzoli<sup>1</sup>, Muhammad Jawad Munawar<sup>4</sup> and Mubashir Ali<sup>1</sup>

<sup>1</sup>Laboratory for Provenance Studies, Department of Earth and Environmental Sciences, University of Milano-Bicocca, Milano, Italy; <sup>2</sup>Department of Earth Sciences, University College London, London, UK; <sup>3</sup>Institute of Marine and Environmental Sciences, University of Szczecin, Szczecin, Poland and <sup>4</sup>Institute of Geology, University of the Punjab, Lahore, Pakistan

#### Abstract

Deserts must be supplied with sediment in order to accrete. The Thar Desert, lying east of the Indus River in South Asia, might be expected to be largely supplied with sediment from that drainage. In this study, we use a combination of major and trace element bulk-sediment geochemistry, together with Sr and Nd isotopes, to constrain the provenance of postglacial dune sand. Our data indicate a stronger influence from mafic source rocks in the Sindh Desert compared to that in Cholistan. Nd isotopes imply sediment was largely derived from the lower Indus River during the early and pre-Holocene post-glacial time. The sand is coarser grained in Sindh and retains higher  $\epsilon_{\rm Nd}$  values in sediment that eroded from mafic rocks in Kohistan and the Karakorum as a result of deflation of deltaic and floodplain areas in the lower reaches by southwesterly summer monsoon winds. The composition of Cholistan dunes, like that in the Eastern Thar Desert, reveals instead more supply from Himalayan sources and more negative  $\epsilon_{\rm Nd}$  values. The greater Himalayan influence in Cholistan and the Eastern Thar Desert largely reflects finer grain size, a result of the longer transport from the delta source and a preference for more Himalayan supply in the form of finer sediment.

## 1. Introduction

Landscape evolution is linked to the interplay of influences over physical erosion and chemical weathering that are in turn governed by tectonics and climate change (Burbank et al. 2003; Gabet & Mudd, 2009; Reiners et al. 2003; Riebe et al. 2004). Changes in these processes result in alteration of sediment compositions that may be preserved in the final depocenter, albeit modulated during transportation along the pathway between source and sink (Allen, 2008; Clift & Jonell, 2021; Kuehl et al. 2016). Sediments may be stored and later released from floodplains and dryland regions, including deserts, which may affect the rate of supply and composition of sediment supply to the final depocenter. Depending on the duration of sediment transport, significant chemical weathering may occur in floodplains along the course between mountainous sources and the lower reaches and river mouth (Lupker et al. 2012). Reworking of floodplain sediments can play a vital role in controlling river sediment composition, as can recycling from desert regions that are proximal to the river (Alizai et al. 2011a; Clift & Jonell, 2021). Erosion patterns and rates are also controlled by tectonic processes that uplift source terrains over millions of years, but here we consider specifically the influence of climate-modulated surface processes changing over orbital and shorter timescales (<10<sup>5</sup> years) (Clift et al. 2010a; Colin et al. 2010; Fildani et al. 2016; Mason et al. 2019).

In Earth's history, changing climate and sediment supply have been factors behind the formation of deserts associated with drainage basins (Blum & Törnqvist, 2000). Deserts are found preferentially at the mid-latitudes, where descending dry air masses lead to increased aridity (Bostock *et al.* 2006; Cronin, 1999). Global climate change can increase the extent and location of arid regions (Zeng & Yoon, 2009). Deserts also form in the rain shadow of tectonically generated mountain ranges (Galewsky, 2009; Garzanti *et al.* 2022) and can potentially accumulate large volumes of detritus that buffer the sediment flux between mountain sources and their final depocenter.

Here, we investigate the associations between the Thar Desert of South Asia, the Indus River and climate change since the Last Glacial Maximum (LGM, ~20 ka) (Fig. 1). The semi-arid Thar Desert of the northwestern Indian subcontinent is affected by the southwesterly summer monsoon, so named because this is the direction of the dominant winds. Thar Desert sediments are predominantly derived from the western Tibetan-Himalaya orogen, with supply from the mainstream Indus River, as well as from its Himalayan tributaries from the east (i.e., Punjab)

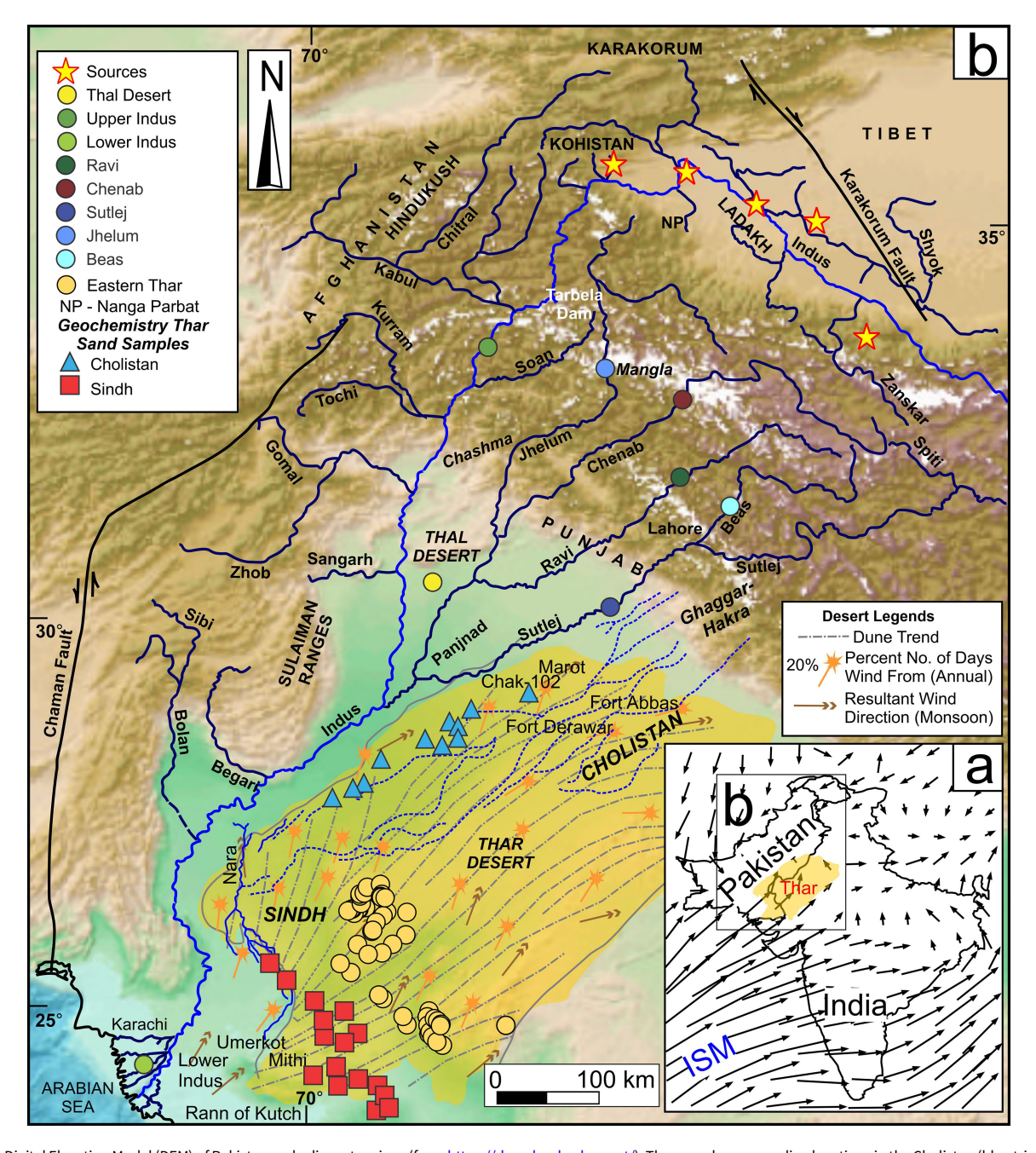


Figure 1. Digital Elevation Model (DEM) of Pakistan and adjacent regions (from https://download.gebco.net/). The map shows sampling locations in the Cholistan (blue triangles) and Sindh (red squares) deserts. In the map, blue curves show major rivers, and dotted curves show palaeorivers in the desert sides, and the map is adapted from Usman et al. (2024).

(Clift *et al.* 2004; Garzanti *et al.* 2005, Usman *et al.* 2024). The main Indus River carries detritus eroded from the Karakorum, Kohistan and Nanga Parbat ranges to the lower reaches (Fig. 1).

The Thar Desert contains aeolian dunes built by monsoon and, to a lesser extent, westerly winds over a variety of timescales (Glennie *et al.* 2002; Kar *et al.* 1998; Singhvi & Kar, 1992). These winds bring rain that is largely focused on the southern flank of the western Himalaya, resulting in high erosion rates (Bookhagen & Burbank, 2006). In this study, we present multi-proxy datasets that test this monsoon-dominated sediment supply model. We employ a series of geochemical and isotopic methods that have been proven to be effective provenance proxies within the Indus River system to constrain the source of sediment in the modern Thar Desert. In particular, we investigate if systematic differences occur

across the northern and southern parts of the western Thar Desert, respectively found in the Pakistani provinces of Cholistan and Sindh, as well as in Indian Rajasthan's Eastern Thar Desert (Bhattacharyya *et al.* 2024) (Fig. 1). Besides utilizing the unique chemical and isotopic signatures of the primary sediment sources as reference, we also consider the role played by other parameters that may influence the composition of dune sand, including grain size and weathering. Contrasting degrees of weathering can be used to constrain the sediment sources, although additional weathering may also occur in floodplains, and it should be remembered that this may change as the monsoon strengthened and declined through time (Clift *et al.* 2008; Clift *et al.* 2010a). More broadly, warmer and more humid conditions enhance chemical alteration and clay mineral formation as a result of the close relationship

between climate and weathering rates (Kump et al. 2000; West et al. 2005).

Chemical alteration results in a loss of water-mobile elements (e.g., Na, K, Ca, Mg, Sr) over immobile elements (e.g., Si, Al, Ti) compared to the original composition and thus allows the intensity of alteration to be quantified (Nesbitt *et al.* 1980). Changing climate also influences the speed and duration of sediment transport between the source and the final depocenter (Herman & Champagnac, 2016; Huntington *et al.* 2006; Neubeck *et al.* 2023; West *et al.* 2005), which in turn influences the degree of alteration that detrital grains encounter. We use a combination of grain-size analysis, bulk-sediment major and trace element geochemistry with Sr and Nd isotopes to investigate the desert sand origin and the processes that have allowed the desert to form.

### 2. Geological evolution and Thar Sand dune accretion

Quaternary aeolian sediment deposits in the Thar Desert are interspersed between low hills of Cenozoic rocks and rest upon a substratum of Archean gneiss covered by Proterozoic sedimentary rocks and recent alluvium. The wind remobilized fluvial sediments and then created sand ridges that characterize the present desert landscape, occasionally separated by interdune clay deposits. Ahmad (2008) had hypothesized that the sand in the northern part of the desert (i.e., in Cholistan) was predominantly derived from the Sutlej River. However, detrital U-Pb zircon dating and Nd isotope data, presented by East et al. (2015), refuted this model by indicating that sediment in the region is sourced from the modern Indus delta. Sediment in the southern desert has been supplied by recycling from the mid-Holocene delta (East et al. 2015). In contrast, studies by Clift et al. (2002), Garzanti et al. (2013b) and Usman et al. (2024) suggested that the southern desert region (i.e., Sindh) sand is primarily sourced from the recent Indus River. Recent analysis of the Eastern Thar Desert in India employed Nd and Sr isotopes to argue that this region is also primarily Indus-supplied (Bhattacharyya et al. 2024), suggesting sediment supply from the exposed Indus Shelf during and immediately after the LGM. The pre-industrial sediment load of the Indus River was large (250-450 Mt/y) (Milliman & Farnsworth, 2011) and could have served as the primary source of sand for the southern reaches of the Thar Desert.

The dynamics of the Indus River and its potential influence on the Thar Desert have been debated over the years. The significant role that river systems play in shaping desert landscapes, particularly in regions where fluvial processes interact with arid environments, has been recognized (Bookhagen & Burbank, 2010; Clift et al. 2012; Clift et al. 2002; Garzanti et al. 2020; Usman et al. 2024). These studies underscored the importance of understanding sedimentary processes within the Indus River basin if their implications for the evolution of adjacent arid regions are to be appreciated. Both climatic variability and tectonic activity modulate sediment fluxes from the Himalayas to the Indus River and ultimately influence depositional patterns in the Thar region (Clift et al. 2008; Tandon & Sinha, 2022). A comprehensive understanding of transport and depositional processes in the Indus River is essential for elucidating its relationship with the Thar Desert.

The arid and hot climate of the Thar Desert (annual summer temperature: 50°C, winter: 10°C and annual rainfall of 100–200 mm) reflects its location between the Himalaya and the adjacent floodplains (Fig. 1). Furthermore, the desert is at the edge of the influence of monsoonal rains (Bookhagen & Burbank, 2006). Previous studies of the Eastern Thar Desert showed that sand dunes have accreted in multiple phases over the last 200,000 years

(Singhvi et al. 2010). Desert expansion is a function of both the amount of sediment supplied and wind intensity carrying material across the region. It might be expected that periods of weak monsoonal rain, such as during the LGM (Clift & Plumb, 2008; Zhisheng et al. 2011), would be periods of desert expansion. However, existing provenance analysis suggests that much of the sediment supply occurred when the summer monsoon was strong, during the end of the LGM and when the climate shifted to become wetter, which highlights the strong monsoonal influence over Thar Desert sedimentation (Clift & Giosan, 2014; East et al. 2015; Garzanti et al. 2020; Glennie & Singhvi, 2002; Singh et al. 1990). A recent re-examination of detrital zircon single-grain U-Pb dates suggests that much of the sediment was supplied from the lower reaches to the desert after the LGM, during the latest Pleistocene, and in the early to mid-Holocene (Usman et al. 2024).

Thermoluminescence dating of aeolian sediments in the Thar Desert has yielded evidence of multiple phases of dune accretion during the past 200 k.y., punctuated by interludes of low or weak sediment supply related to orbital precessional forcing (Nitundil et al. 2023; Singhvi et al. 2010). The last major phase of dune growth in the Eastern Thar Desert took place during a transitional climate, when the southwesterly monsoon winds were strengthening following an aridity peak during the LGM (Gebregiorgis et al. 2016; Srivastava, 2023). Sand aggradation in the Eastern Thar Desert started between 17 ka and 14 ka and lasted until 9 ka, at the onset of the early Holocene wet phase (Dhir et al. 2010; Singhvi et al. 2010). In contrast, the western Thar Desert is argued to have been supplied by Indus Delta sediment since the onset of wetter, windier conditions during the Holocene (Usman et al. 2024). The desert has expanded further towards the west as the climate dried following the mid-Holocene, potentially bringing it into proximity with the Indus River (Alizai et al. 2011a; East et al. 2015).

Although the subsidence of the Himalayan foreland requires the Indus River to flow in the deepest part of this flexural basin, there has been some evolution of the river courses through time. The delta itself has migrated to the west since the early Holocene and appears to have reached the sea near the Rann of Kutch (Fig. 1) early in the Holocene, before moving to its modern location (Inam et al. 2007). It is possible that the lower Indus used to flow through the Nara Valley, west of its present course, but provenance work was unable to resolve between this possible earlier course and infilling of a separate channel by Thar Desert sands (Alizai et al. 2011b). Further north, the location where the Indus and its Himalayan tributaries reached the flood plains has been stable since they are fixed in deep rocky gorges, although there is evidence for the migration of the Sutlej to the NW to its modern location during the Holocene (Mehdi et al. 2016; Saini et al. 2009) and the cessation of flow in an ephemeral Ghaggar-Hakra stream by ~4-8 ka (Clift et al. 2012; Khan et al. 2024). Although the Yamuna used to flow to the west into the Indus in the past, this connection was likely lost before ~20 ka (Clift et al. 2012).

#### 3. Methods

## 3.a. Grain size and geochemical analyses

The grain-size distribution of 27 sand samples (collected from the surface of sand dunes in the Western Thar Desert (Sindh and Cholistan, Pakistan)) was quantified at the University of Milano-Bicocca by employing standard wet sieving techniques; textural parameters were recalculated using the Folk & Ward (1957) classification (Table 1). For geochemical analysis, samples were

Table 1. Grain-size analyses of studied samples and major-element distribution in aeolian sand of the Sindh and Cholistan deserts are determined by X-ray fluorescence, with different weathering proxies

Desert	Site	Sample	Mean grain size (μm)	SiO <sub>2</sub> (wt%)	Al <sub>2</sub> O <sub>3</sub> (wt%)	Fe <sub>2</sub> O <sub>3</sub> (wt%)	MgO (wt%)	TiO <sub>2</sub> (wt%)	CaO (wt%)	Na <sub>2</sub> O (wt%)	K <sub>2</sub> O (wt%)	P <sub>2</sub> O <sub>5</sub> (wt%)	MnO (wt%)	LOI	CIA*	PIA	WIP	Mg/Al (mol)	K/Al (mol)	K/Rb (mol)
Sindh	NE Chotiari	S5986	173	71.7	9.2	1.7	0.8	0.3	4.2	2.0	1.9	0.2	0.0	5	51	40	47	0.2	0.2	290
Sindh	NE Khipro	S5990	236	64.5	6.7	1.5	0.3	0.2	7.4	1.2	1.6	0.2	0.0	5	54	25	44	0.1	0.3	271
Sindh	N Naya Chor	S5996	174	68.0	5.3	1.2	0.7	0.2	8.9	1.3	1.7	0.1	0.0	3	46	16	51	0.3	0.4	344
Sindh	Sajan Jo Par	S5998	174	67.3	8.6	1.9	1.4	0.3	6.0	1.5	1.7	0.1	0.0	3	55	34	47	0.4	0.2	297
Sindh	Ratnaur Road	S6002	181	65.0	10.5	4.0	2.0	0.7	7.5	1.6	1.7	0.3	0.1	4	59	36	53	0.5	0.2	321
Sindh	Chhapar	S6006	157	68.5	10.2	2.6	1.0	0.4	5.8	1.8	1.8	0.1	0.1	4	57	38	49	0.3	0.2	285
Sindh	Kantio	S6008	173	63.3	10.1	3.0	2.2	0.4	8.4	1.8	1.9	0.2	0.1	4	56	31	59	0.6	0.2	326
Sindh	Chachro	S6010	147	64.9	8.8	2.2	1.0	0.4	6.9	1.5	1.8	0.1	0.1	3	56	32	49	0.3	0.2	288
Sindh	E Mithi	S6012	159	61.8	9.1	2.8	0.8	0.4	7.1	1.5	1.9	0.2	0.1	4	57	32	49	0.2	0.2	325
Sindh	W Arniyaro	S6017	162	64.9	9.8	2.7	1.2	0.3	6.6	1.4	2.0	0.1	0.1	3	59	35	50	0.3	0.2	321
Sindh	Khakhanhar	S6019	168	68.6	9.7	2.0	0.8	0.3	6.2	1.9	1.8	0.1	0.0	4	54	35	51	0.2	0.2	273
Sindh	Ade Ka Tar	S6023	163	65.4	9.8	2.8	1.5	0.5	5.7	2.3	1.7	0.1	0.1	4	51	36	55	0.4	0.2	276
Sindh	SE Bhaiwah	S6026	169	62.5	10.2	3.5	2.6	0.4	9.1	1.9	1.7	0.1	0.1	3	56	30	62	0.7	0.2	268
Sindh	NW Virawah	S6029	197	62.0	8.5	2.5	1.5	0.3	8.9	1.9	1.6	0.1	0.1	5	52	26	57	0.4	0.2	266
Sindh	N Sardharo	S6031	169	69.2	9.7	2.4	1.4	0.3	5.5	2.1	1.8	0.1	0.1	6	52	37	52	0.4	0.2	264
Sindh	S Ghartiari	S6034	141	69.7	10.5	2.2	1.2	0.3	4.9	2.1	1.9	0.1	0.1	4	54	41	51	0.3	0.2	277
Cholistan	Kandera	S6112	152	63.6	9.7	3.9	1.4	0.6	6.3	1.8	1.5	0.1	0.1	4	57	37	49	0.4	0.2	240
Cholistan	Monza Lunda	S6117	135	68.8	9.5	2.0	0.9	0.3	3.5	2.0	1.8	0.1	0.0	2	53	45	44	0.2	0.2	265
Cholistan	Basti Baloch	S6120	129	69.1	9.6	2.4	1.2	0.4	4.4	2.2	1.7	0.1	0.1	3	52	40	49	0.3	0.2	242
Cholistan	Abdullah Wali	S6124	137	67.3	9.5	2.3	1.0	0.3	6.0	2.0	1.7	0.0	0.1	4	53	35	51	0.3	0.2	238
Cholistan	Ahmedpur	S6126	116	69.8	9.7	2.2	1.1	0.3	5.0	2.4	1.7	0.1	0.0	5	50	38	52	0.3	0.2	240
Cholistan	Ahmedpur	S6130	139	69.9	10.3	3.0	0.4	0.5	3.4	2.5	1.6	0.1	0.1	2	51	46	46	0.1	0.2	239
Cholistan	Yazman Bijnot	S6133	158	71.0	9.7	2.2	0.5	0.4	2.8	2.7	1.7	0.1	0.0	2	48	46	47	0.1	0.2	245
Cholistan	Yazman	S6135	147	68.4	9.7	2.4	0.5	0.3	3.1	2.7	1.7	0.2	0.1	2	48	45	47	0.1	0.2	260
Cholistan	Yazman Mandi	S6138	113	69.1	9.8	2.2	0.7	0.4	3.9	2.7	1.8	0.1	0.0	2	48	41	52	0.2	0.2	262
Cholistan	Kandera	S6140	93	66.0	9.8	2.6	1.3	0.5	4.8	2.7	1.7	0.2	0.1	3	48	38	55	0.3	0.2	244
Cholistan	Hasilpur	S6142	91	67.4	9.5	2.4	1.0	0.5	2.9	2.3	1.8	0.1	0.0	2	50	46	46	0.3	0.2	248

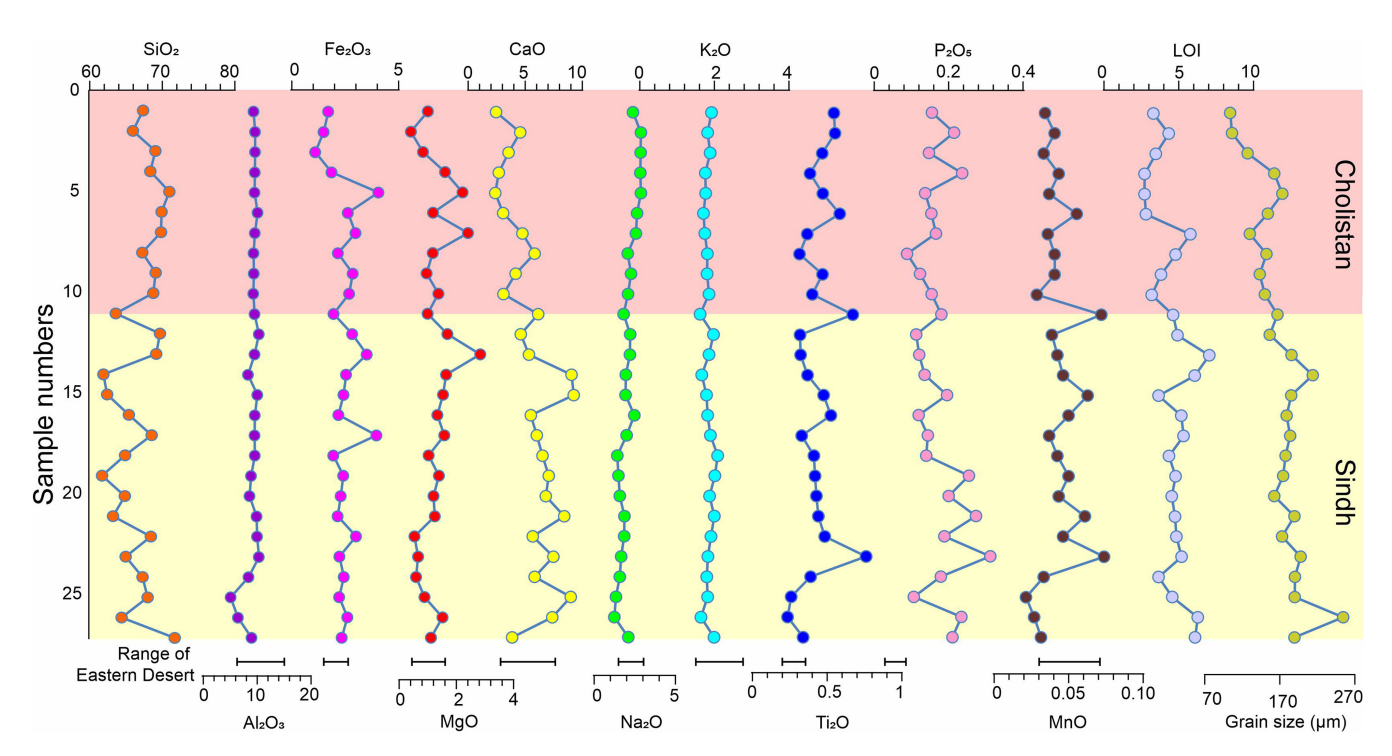


Figure 2. Diagram showing major-element variability and grain-size characteristics of studied aeolian-dune sediments from the Sindh and Cholistan deserts. The range from the Eastern Thar Desert is from Bhattacharyya et al. (2024).

ground in a mortar and then loaded into a hardened steel vial and milled to a grain size of  $<30~\mu m$  using a SPEX Sample Prep 8000M Mixer/Mill. Approximately 2.00  $\pm$  0.02 g of powder from each sample was weighed and loaded into a furnace at 900°C for two hours. Following extraction from the furnace, the sample powders were re-weighed and their loss on ignition (LOI) calculated. Geochemical analysis was conducted with a Bruker S2-PUMA energy-dispersive X-ray fluorescence (XRF) instrument at the Chevron Geomaterials Characterization Laboratory at Louisiana State University (LSU), after calibration against 19 international standards. Analytical uncertainties calculated as a percentage of the content were ~15% for Na\_2O and <2% for the other elements, reflecting the higher volatility and mobility of Na during analysis. The results are presented in Tables 1 and 2.

## 3.b. Sr and Nd Isotopes

Sr and Nd isotopes have been widely used as provenance proxies (Goldstein et al. 1984) and were also found to be successfully effective in the Indus River system (Clift et al. 2002). Their contents were measured in 11 representative powdered bulksediment samples based on geochemical content. After decarbonation with 10% acetic acid and dissolution, Sr and Nd were concentrated by standard column extraction techniques, and isotopic compositions were measured by the Thermo 'Neptune' multi-collector inductively coupled plasma mass spectrometer (MC-ICP-MS) at the Woods Hole Oceanographic Institution. Analytical methods are described in the Supplementary Information. However, analytical uncertainties are extremely low, and Jonell et al. (2018) noted that within the Indus drainage system, bulk isotopic compositions may vary up to ±1.04 units for  $\varepsilon_{Nd}$  and  $\pm 0.0099$  for  $^{87}Sr/^{86}Sr$  values in any sediment because of mineralogy and grain size distribution. This real-world

uncertainty is much greater than the analytical error. The results are presented in Table 3.

## 4. Geochemical variability of the Thar Desert

#### 4.a. Major and trace elements

The variability of major-element concentrations in Thar dune sand is moderate. SiO $_2$  (Sindh 62–72%; Cholistan 64–71%), Al $_2$ O $_3$  (Sindh 5–10%, Cholistan 9–10%), Fe $_2$ O $_3$  (Sindh 5–10%, Cholistan 9–10%), MgO (Sindh 5–10%, Cholistan 9–10%), CaO (Sindh 5–10%, Cholistan 9–10%), Na $_2$ O (Sindh 1–2%, Cholistan 2–3%), K $_2$ O (Sindh 1.5–1.8%, Cholistan 1.6–2.0%), TiO $_2$  (Sindh 0.2–0.7%, Cholistan 0.3–0.6%), P $_2$ O $_5$  (Sindh 0.1–0.3%, Cholistan 0–0.2%) and MnO (Sindh and Cholistan <0.1%) (Fig. 2). Such chemical variability is partly grain-size dependent. Sindh dune sand is significantly coarser than Cholistan sand and has mainly lower SiO $_2$  content (Fig. 3a) and higher CaO (Fig. 3b). Differences and significant variabilities in the distribution of major oxides between Cholistan and Sindh desert sands, together with their correlation trends, are illustrated in Figure S1.

In general, Sindh Desert sand is richer in Sr, S, V, Cr, Nb and Sb than that from Cholistan. Trace element contents of Thar Desert sand do not show major systematic differences with both the Indus and Himalayan tributary sands (Fig. 4b). Normalizing trace-element concentration against the Upper Continental Crust (UCC) (Taylor & McLennan, 1995) allows us to compare the Thar Desert sands with the signatures of Upper and Lower Indus sediments together with Himalayan tributary sands determined by earlier studies (Garzanti *et al.* 2020; Liang *et al.* 2019) (Figs. 4a, 4b). Analyses from the Eastern Thar Desert (Bhattacharyya *et al.*, 2024) do not include as many elements as provided by this work, but when comparison is possible, the different sands are seen to be similar, except that Zr contents are much lower in the east (Fig. 4a).

Table 2. Trace-element distribution with alpha values normalized to non-mobile Al calculated in aeolian sand of the Sindh and Cholistan deserts determined by X-Ray Fluorescence

												Trac	ce Ele	emen	ts											Alpha I	ndices		
Desert	Site	Sample	Mean grain size (μm)	Sr	Rb	S	٧	Cr	Ni	Cu	Zn	Ga	As	Υ	Zr	Nb	Мо	Cd	Sb	Ва	La	Pb	Th	$\alpha^{Al}$ Na	$\alpha^{Al}Ca$	$lpha^{Al}Sr$	$\alpha^{Al} Mg$	$\alpha^{Al}K$	α <sup>Al</sup> Ba
Sindh	NE Chotiari	S5986	173		59		48	18	10	4	40	13	3	15	108	8	0	0	0	346	11	16	4	1.1	0.6	-	1.7	1.0	1.0
Sindh	NE Khipro	S5990	236		52		32	22	9	9	41	12	2		160	34	0	0	1	274	9	30	8	1.3	0.2	-	3.8	0.9	0.9
Sindh	N Naya Chor	S5996	174	397	45	397	27	22	12	4	34	7	3	9	85	8	1	0	2	334	9	16	7	0.9	0.2	0.3	1.2	0.6	0.6
Sindh	Sajan Jo Par	S5998	174		52		24	19	7	7	16	8	1	16	132	12	0	0	1	359	17	34	8	1.3	0.4	-	0.9	1.0	0.9
Sindh	Ratnaur Road	S6002	181	549	49	549	85	76	20	4	46	13	2	36	244	7	1	0	1	324	15	15	12	1.5	0.4	0.4	0.8	1.2	1.2
Sindh	Chhapar	S6006	157	774	58	774	45	75	17	9	42	14	3	21	126	7	1	0	1	334	7	9	9	1.3	0.4	0.3	1.5	1.1	1.2
Sindh	Kantio	S6008	173	1034	53	1034	58	81	12	3	36	9	1	25	111	9	1	0	1	372	9	11	12	1.3	0.3	0.2	0.7	1.1	1.0
Sindh	Chachro	S6010	147	1034	56	1034	31	29	11	6	41	9	3	18	111	8	1	1	1	347	8	32	10	1.3	0.3	0.2	1.3	1.0	1.0
Sindh	E Mithi	S6012	159	876	53	876	43	71	16	7	58	11	4	17	134	12	1	0	1	349	8		10	1.5	0.3	0.2	1.7	1.0	1.0
Sindh	W Arniyaro	S6017	162	451	56	451	59	74	14	7	42	8	2	20	131	8	1	0	1	388	19	10	10	1.6	0.4	0.5	1.2	1.0	1.0
Sindh	Khakhanhar	S6019	168	188	60	188	39	121	15	6	37	13	2	16	94	8	0	0	1	333	10	15	5	1.2	0.4	1.1	1.8	1.1	1.1
Sindh	Ade Ka Tar	S6023	163	157	57	157	42	170	16	14	33	12	1	23	182	11	0	0	1	376	11	24	8	1.0	0.4	1.4	1.0	1.1	1.0
Sindh	SE Bhaiwah	S6026	169	262	57	262	71	218	15	4	44	17	2	25	129	9	1	0	1	363	13	4	8	1.3	0.3	0.9	0.6	1.2	1.1
Sindh	NW Virawah	S6029	197	169	54	169	26	128	15	4	36	15	2	16	100	9	0	0	1	374	5	26	6	1.1	0.2	1.1	0.9	1.1	0.9
Sindh	N Sardharo	S6031	169	246	61	246	36	227	16	4	38	11	2	18	99	5	0	0	1	347	12	16	8	1.1	0.4	0.9	1.1	1.1	1.1
Sindh	S Ghartiari	S6034	141	204	61	204	40	166	19	6	30	14	1	16	87	6	1	0	1	372	12	25	3	1.2	0.5	1.1	1.4	1.1	1.1
Cholistan	Kandera	S6112	152	122	58	122	65	40	18	10	59	13	3	33	223	8	0	1	1	418	20	17	13	1.3	0.4	1.7	1.1	1.3	0.9
Cholistan	Monza Lunda	S6117	135		60		19	52	16	1	43	13	2	19	92	5	0	0	0	389	12	27	5	1.1	0.7	-	1.7	1.1	0.9
Cholistan	Basti Baloch	S6120	129	145	64	145	28	53	8	8	43	15	2	20	132	7	1	1	1	396	23	20	7	1.0	0.5	1.5	1.2	1.1	0.9
Cholistan	Abdullah Wali	S6124	137	168	65	168	44	52	14	4	40	14	3	17	117	8	0	0	1	433	19	14	7	1.1	0.4	1.2	1.4	1.1	0.8
Cholistan	Ahmedpur	S6126	116	405	62	405	57	22	10	9	49	14	9	21	156	10	1	2	1	426	11	8	7	0.9	0.5	0.5	1.4	1.2	0.9
Cholistan	Ahmedpur	S6130	139	71	61	71	27	23	14	7	62	15	12	21	162	13	1	1	1	417	13	13	6	1.0	0.8	3.2	4.0	1.3	0.9
Cholistan	Yazman Bijnot	S6133	158	79	62	79	34	22	14	5	41	16	4	16	132	12	1	2	0	354	10	30	5	0.8	0.9	2.7	2.9	1.2	1.1
Cholistan	Yazman	S6135	147	236	58	236	33	19	15	5	56	18	12	17	123	14	1	1	0	399	6	15	7	0.9	0.8	0.9	3.3	1.2	0.9
Cholistan	Yazman Mandi	S6138	113		62		25	15	11	7	56	11	13	17	135	13	0	3	0	408	10	19	7	0.9	0.6	-	2.1	1.1	0.9
Cholistan	Kandera	S6140	93		64		36	14	15	10	52	18	8	21	213	20	1	4	1	394	8	33	5	0.8	0.5	-	1.1	1.1	1.0
Cholistan	Hasilpur	S6142	91		67		27	20	13	9	45	13	4	22	162	13	0	1	0	336	4	45	7	1.0	0.8	-	1.5	1.1	1.1

**Table 3.**  $^{87}$ Sr/ $^{86}$ Sr and  $^{143}$ Nd/ $^{144}$ Nd isotopic ratios determined by Thermo the 'Neptune' multi-collector inductively coupled plasma mass spectrometer (MC-ICP-MS) at Woods Hole Oceanographic Institution

Desert	Site	Sample	<sup>87</sup> Sr/ <sup>86</sup> Sr	<sup>143</sup> Nd/ <sup>144</sup> Nd	$\epsilon_{Nd}$
Sindh	NE Chotiari	S5986	0.71769	0.51215	-9.60
Sindh	N Naya Chor	S5996	0.72038	0.51212	-10.03
Sindh	Chhapar	S6006	0.72245	0.51215	-9.52
Sindh	Chachro	S6010	0.72168	0.51201	-12.21
Sindh	Khakhanhar Bajeer	S6019	0.71958	0.51215	-9.60
Sindh	SE Bhaiwah	S6026	0.72410	0.51212	-10.18
Sindh	S Ghartiari	S6034	0.72528	0.51212	-10.05
Cholistan	Kandera	S6112	0.72235	0.51204	-11.76
Cholistan	Basti Baloch	S6120	0.72593	0.51204	-11.72
Cholistan	Ahmedpur	S6126	0.72253	0.51202	-11.98
Cholistan	Yazman Bijnot	S6133	0.72479	0.51200	-12.39
Cholistan	Yazman	S6135	0.72326	0.51205	-11.55
Cholistan	Hasilpur	S6142	0.73087	0.51192	-13.99

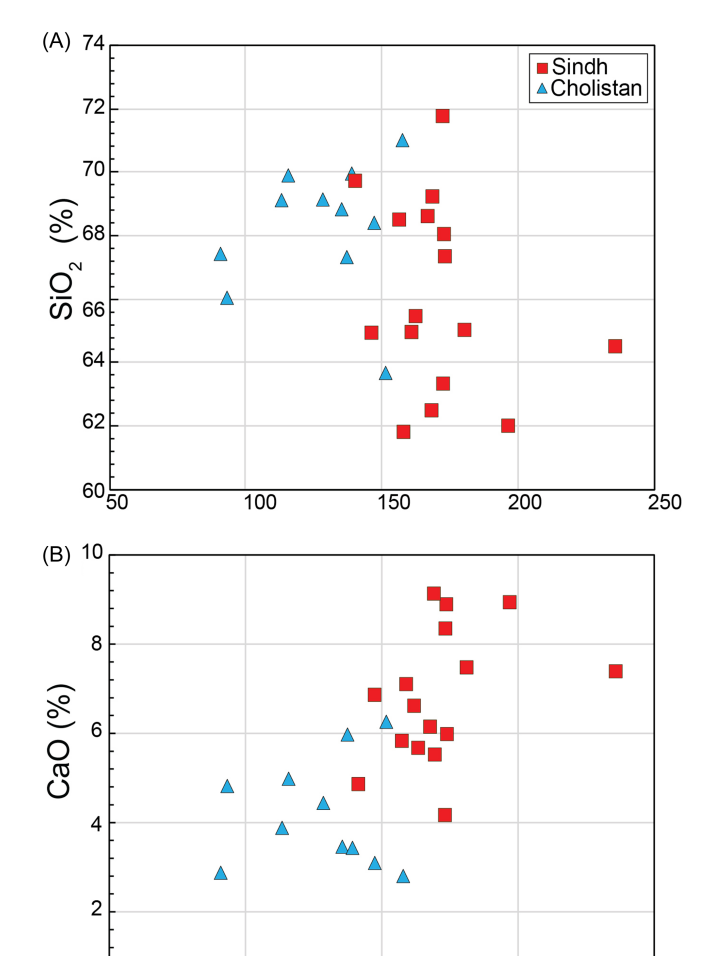


Figure 3. Cross-plots showing that Sindh Desert sand is coarser but has lower  $SiO_2$  (A) and higher CaO (B) than Cholistan Desert sand.

150

Mean grain size (µm)

\_ 250

#### 4.b. Sr and Nd Isotopes

Sindh Desert sand yields generally less negative  $\epsilon_{\rm Nd}$  (-9.0 to -12.0) values compared to the Cholistan sand (-11.8 to -14.0) (Fig. 5), which also has slightly higher  $^{87}{\rm Sr}/^{86}{\rm Sr}$  values (0.71769 to 0.72528 in Sindh versus 0.72235 to 0.73087 in Cholistan). Sindh Desert sand also has less negative  $\epsilon_{\rm Ngrd}$  values compared to the Holocene Indus post-LGM delta ( $\epsilon_{\rm Nd}$  values of -11.8 to -10.8 before 12 ka) (Clift *et al.* 2010b). In comparison with potential source regions, Thar Desert sands are similar to Holocene Indus River and delta sands ( $\epsilon_{\rm Nd}$  values of -12.9 to -15.4 since 9 ka) (Clift *et al.* 2008), with intermediate values between Karakorum and Himalayan endmember sources (Fig. 5).

## 5. Compositional signatures of the Thar Desert

The geochemical signatures of the Thar Desert sands (Fig. S2a) are here compared with those of mainstream Indus River sediments and its Himalaya-draining Punjabi tributaries (Fig. S2b) and details in Table 4. Sindh Desert sands are similar to the lower Indus River and the Indus in Ladakh, India. Himalayan-derived river sediment contains significantly less CaO and more Na<sub>2</sub>O and TiO<sub>2</sub> than the Sindh average. Cholistan sands are similar to the Himalayan bedrock and the Sutlej River, especially with regard to Ni, Cu, Zn, Al<sub>2</sub>O<sub>3</sub> and Ga contents. As far as grain size is concerned, Sindh dunes tend to be coarser-grained than Cholistan dunes (Fig. 3), which is ascribed to deflation by strong southwesterly summer monsoon winds that blow sand from the Indus delta inland (East et al. 2015; Usman, 2024; Usman et al. 2024). On the contrary, the prevalence of finer-grained sediments in Cholistan dunes is attributed to a significant amount of detritus supplied by Himalayan rivers.

## 5.a. Geochemical proxies and grain size in the Thar Desert

Geochemical indices are widely used to estimate weathering intensity (Price, 1995; Minyuk *et al.* 2014; Duzgoren-Aydin & Aydin, 2003; Bloemsma et al. 2012; Guo et al. 2021: Maslov & Podkovyrov, 2023; Price & Velbel, 2003), even though these proxies are also strongly controlled by grain size, source-rock lithology and hydraulic sorting (Dinis *et al.* 2017; Garzanti & Resentini, 2016). The Chemical Index of Alteration (CIA) (Nesbitt & Young, 1982) is widely used and is calculated from molar proportions with the following equation:

$$CIA = (Al_2O_3/(Al_2O_3 + CaO + NaO + K_2O)) * 100$$

CIA only considers CaO hosted in silicate minerals (if the number of CaO moles after correcting for CaO in phosphate is greater than that of Na<sub>2</sub>O, CaO in silicates can be assumed as = Na<sub>2</sub>O; CIA\*, (McLennan, 1993)). CIA values for unweathered source rocks range from 30–40 for basalt to 45–55 for granite and granodiorite, whereas they are 75–85 for illite, ~75 for muscovite, and ~100 for kaolinite and chlorite.

An alternative proxy is the weathering index of Parker (1970) (WIP). WIP is calculated with the following molar equation:

$$WIP = \left(\frac{2Na_2O}{0.35} + \frac{MgO}{0.9} + \frac{2K_2O}{0.25} + \frac{CaO}{0.7}\right) * 100$$

Other geochemical indices have also been used as proxies to track weathering intensity, e.g., K/Al and K/Rb (Nesbitt & Young, 1982; Price & Velbel, 2003). However, all such proxies are also

100

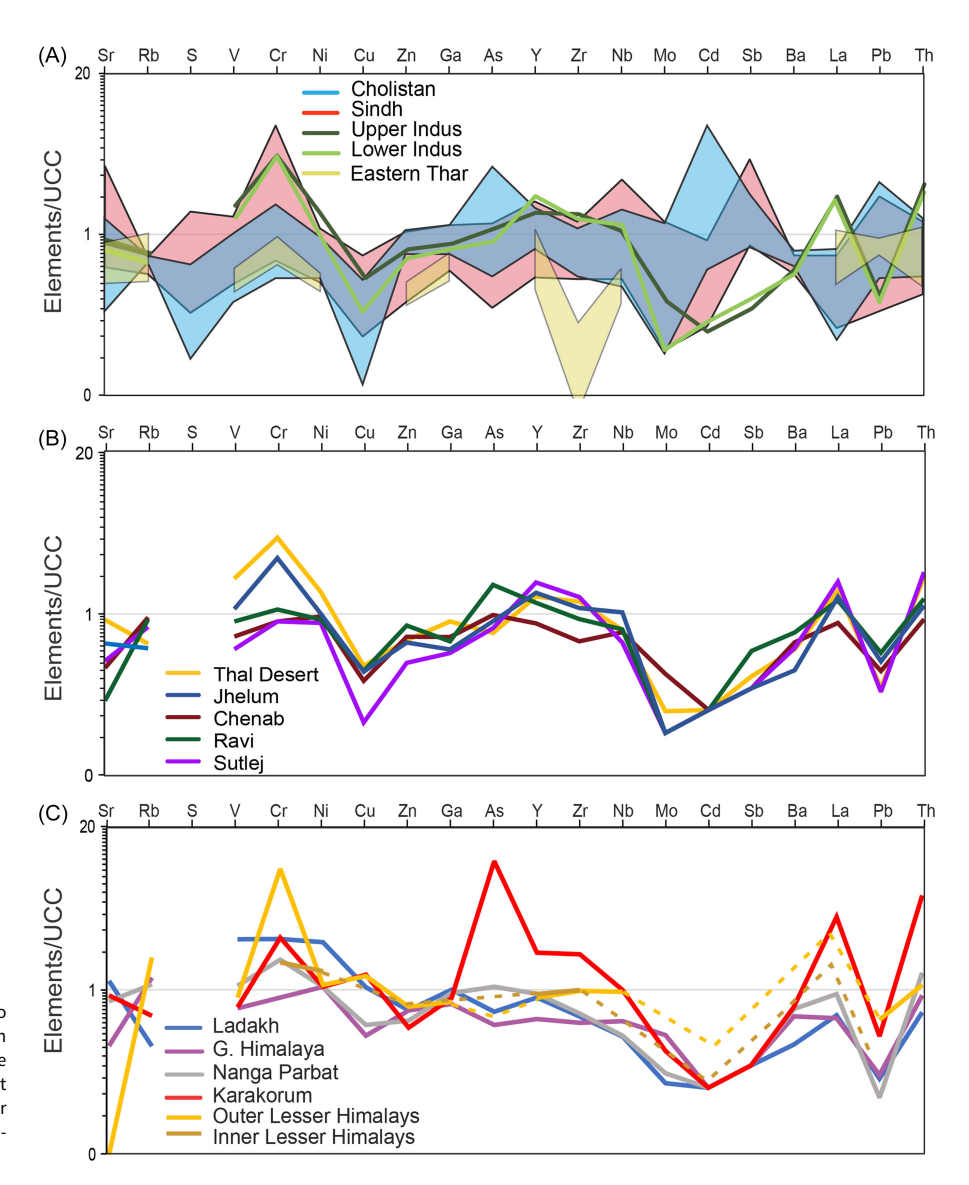


**Figure 4.** Trace element compositions normalized to the Upper Continental Crust (UCC) standard for (**A**) Sindh and Cholistan dune sand, compared with sand of the Upper and Lower Indus River and Eastern Thar Desert (Bhattacharyya *et al.* 2024); (**B**) the Thal Desert and major Punjabi tributaries; and (C) river sands derived from endmember sources (data from Garzanti *et al.* (2020)).

partially controlled by grain size (von Eynatten et al. 2012; von Evnatten et al. 2016), hydraulic sorting or quartz addition by recycling of older sediments (Fig. 6). Rb is not as water-immobile as Al, but it is less water-mobile than K in micas and K-feldspar grains (Nesbitt et al. 1997). K/Rb has been used to effect in several studies in Asia and was tested against an array of environmental proxies by Hu et al. (2016) in a synthesis that showed K/Rb to be more sensitive to chemical weathering than K/Al, at least in the Pearl River. There is a common relationship between different weathering proxies (e.g., CIA\*, K/Al, K/Rb) and mean grain size, because finer sediments are generally expected to show a higher degree of alteration. Coarser sediments tend to have higher CIA\* values (Fig. 6a), implying a stronger control by source-rock lithology and sediment recycling rather than weathering over this proxy. Eastern Thar sediments plot closest to Sindh sediments (Fig. 7) in being coarser and having higher CIA\* values and even exceed these, trending towards Himalayan tributary or Upper Indus sediment compositions. Finer-grained Thar sediments have a lower K/Rb ratio (Fig. 6b), indicating that this proxy may be more sensitive to grain size. Finally, no relationship is observed between LOI, which is expected to be higher when alteration is greater, and grain size (Fig. 6c).

Chemical weathering proxies (e.g., CIA\*, K/Al, Mg/Al) have different sensitivities to weathering intensity, which reflects the mineralogy of the sediment sources and the relative mobility of the elements within them (Hu *et al.* 2016). We compare the different weathering proxies by cross-plotting them against one another. In both Sindh and Cholistan, high Mg/Al is correlated with low CIA\* (Fig. 6d). This implies that Mg/Al is not primarily a weathering proxy but is linked to the influence of Mg-rich mafic rocks widely exposed in Kohistan and the Karakorum.

## 5.b. Provenance versus weathering effects

The Thar Desert sands are mostly enriched in the Ca-Na endmember in the (Ca+Na)-Al-K diagram (Nesbitt & Young, 1989) (Fig. 7a), reflecting the prevalence of plagioclase over K-feldspar in the sources. Average CIA values (51 for Cholistan sand, 54 for Sindh sand) indicate low weathering intensity. Sediments from the Holocene Indus Canyon (Li *et al.* 2018) and post-glacial Indus Delta (Clift *et al.* 2010a) are finer grained than Thar Desert sand and show higher CIA indices. The Al<sub>2</sub>O<sub>3</sub>/SiO<sub>2</sub> ratio, which is often used as a grain-size proxy, and the Fe<sub>2</sub>O<sub>3</sub>/SiO<sub>2</sub> exhibits a wide variation in Indus River sediments (Fig. 7b). Holocene and modern

**Table 4.** Comparison of geochemical, isotopic, mineralogical and provenance features of sediments from the Sindh Desert, Cholistan Desert and potential sediment sources (Upper Indus, Punjab tributaries, Indus Delta). The dataset integrates major and trace element geochemistry, Sr–Nd isotopic signatures, mineralogy, detrital zircon U–Pb age spectra and weathering proxies, highlighting compositional overlaps and contrasts that help discriminate source contributions and post-depositional processes

Feature	Sindh Desert	Cholistan Desert	Upper Indus	Punjab Tributaries	Indus Delta (Holocene/ Post-LGM)
Major Elements	Lower SiO <sub>2</sub> , higher CaO; richer in Sr, S, V, Cr, Nb, Sb	Higher Al <sub>2</sub> O <sub>3</sub> , Fe <sub>2</sub> O <sub>3</sub> , MgO; higher Na <sub>2</sub> O, TiO <sub>2</sub>	Lower CaO, higher Na <sub>2</sub> O & TiO <sub>2</sub>	High Al <sub>2</sub> O <sub>3</sub> , Ga, Ni, Cu, Zn	Variable: enriched in quartz, finer grained
Trace Elements	Comparable to Indus; enriched Sr, Cr, Nb	Similar to Sutlej & Himalayan rocks	Enriched mafic element signal (Mg, Cr)	Depleted relative to UCC; recycling signature	Holocene sediments enriched vs. Lower Indus
Sr-Nd Isotopes	$e_{Nd} = -9.0 \text{ to } -12.0;  ^{87}\text{Sr}/$ $^{86}\text{Sr} = 0.717 - 0.725;  \text{close to}$ Upper Indus (Tarbela)	$\varepsilon_{\mathrm{Nd}}=$ -11.8 to -14.0; <sup>87</sup> Sr/ $^{86}$ Sr = 0.722–0.731; overlaps with Holocene delta	$\epsilon_{Nd}$ less negative (primitive signature)	More negative $\epsilon_{Nd}$ values	Holocene delta $\epsilon_{Nd} =$ -12.9 to -15.4; post-LGM slightly less negative
Mineralogy	Litho-feldspatho-quartzose; more sedimentary lithics; richer in heavy minerals (pyroxene, hornblende, garnet)	Feldspatho-litho-quartzose; more quartz, more metamorphic lithics	Mafic-rich (Kohistan, Karakorum)	Dominated by Himalayan detritus, less pyroxene	Enriched in quartz, depleted in pyroxene
Detrital Zircon U-Pb Ages	Mix of Paleozoic, Neoproterozoic + younger Karakorum/Transhimalayan (Cretaceous-Miocene)	Greater proportion of Himalayan (Proterozoic) grains	Transhimalayan arcs (43–96 Ma; 130–99 Ma, 43–24 Ma)	Greater Himalaya, Lesser Himalaya, Nanga Parbat	Mixed signal; enriched in recycled grains
Weathering Proxies (CIA, K/AI, K/Rb, $\alpha^{\rm Al}$ E)	CIA ~54; low-moderate weathering; $\alpha$ AlCa = 0.2–0.6	CIA ~51; slightly less weathered; $\alpha^{Al}$ Sr = 0.5-3.2	Higher CIA values; finer grained	More weathered than Sindh/ Cholistan; high CIA	Higher CIA than Thar sands

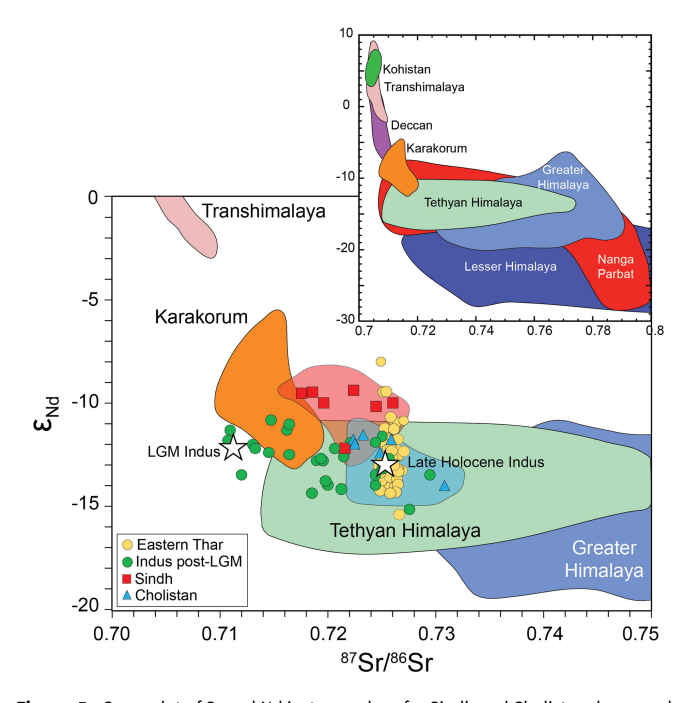


**Figure 5.** Cross-plot of Sr and Nd isotope values for Sindh and Cholistan dune sands compared to end-member sources and post-15 ka Indus Delta sediments (Garzanti *et al.* 2020). Data sources: Transhimalayan: Rolland *et al.* (2002), Singh *et al.* (2002) and Khan *et al.* (1997); Greater Himalaya: Ahmad *et al.* (2000), Deniel *et al.* (1987), Inger *et al.* (1993) and Parrish & Hodges (1996); Karakorum: Crawford & Searle (1992) and Schärer *et al.* (1990); Eastern Thar Desert: Bhattacharyya *et al.* (2024).

river sediments are invariably enriched in quartz relative to their sources and this enrichment is more pronounced in sediments of the Indus delta and the Thar Desert, especially the Sindh Desert. Weathering indices such as the CIA or WIP indicate a slightly higher of weathering intensity for sand carried by the Himalayan Punjabi tributaries and the upper Indus than eolian sediments in the Sindh, Cholistan and eastern deserts (Fig. 7c).

The weathering effect is best resolved from other controls over geochemical composition if mobile elements (e.g., Na, Ca, Sr, Mg, K and Ba) are considered individually (Table 2). This can be done by using  $\alpha^{Al}E$  values, defined as (Al/E)<sub>sample</sub>/(Al/E)<sub>UCC</sub> (Garzanti et al. 2014a; Garzanti et al. 2014b), a parameter that compares the concentration of any mobile element E with reference to nonmobile Al in our samples compared to the UCC. Aluminium, which is hosted in a wide range of rock-forming minerals, including phyllosilicates (concentrated in mud) and feldspars (concentrated in sand), is used as a reference for all elements rather than Ti, Nd, Sm or Th (Gaillardet et al. 1999). Those immobile elements are preferentially hosted in ultra-dense minerals and may thus reach anomalous concentrations as a result of hydrodynamic processes (Garzanti et al. 2013a; Garzanti et al. 2013b).

Sediments from the Thar Desert, Indus River and its Punjabi tributaries show a weak depletion in highly mobile Na ( $\alpha^{Al}$ Na 0.9 to 1.6 in Sindh and 0.8 to 1.3 in Cholistan) compared to the Indus River (Fig. 8a, b). Cholistan and Eastern Thar Desert sands are enriched in Ca, Sr and Mg compared to the Indus, while Sindh sands are generally more depleted than the other desert areas and the Indus, except in regard to Mg.  $\alpha^{Al}$ Ca = 0.2–0.6 and 0.4–0.9,  $\alpha^{Al}$ K = 0.6 -1.2 and 1.1-1.3,  $\alpha^{Al}Sr = 0.2-1.4$  and 0.5-3.2 and  $\alpha^{Al}Mg = 0.6-3.8$ and 1.1-4.0 in Sindh and Cholistan sands, respectively. Instead, Ba is more strongly depleted in both western and eastern deserts ( $\alpha^{Al}$ Ba 0.6–1.2). The Thar Desert has comparable  $\alpha^{Al}E$  values to many of the Himalayan tributaries, except for the Ravi, which is enriched in Na, Ca and Sr. The variability between the Sindh and Cholistan deserts in concentration factors indicates differences in the weathering influence (Viers et al. 2009); however, the lower  $\alpha^{Al}E$ values in Sindh imply stronger weathering.

To explore these conclusions further, we have used the cross plot of K/Si versus Al/Si (Lupker *et al.* 2012) (Fig. 9). We compare the Indus and Thar Desert sediments with material from the Indus Canyon (Li *et al.* 2018) and Indus Delta (Clift *et al.* 2010a) to understand the weathering intensity while accounting for grain size effects. Weathering intensity affects the gradient of the array,

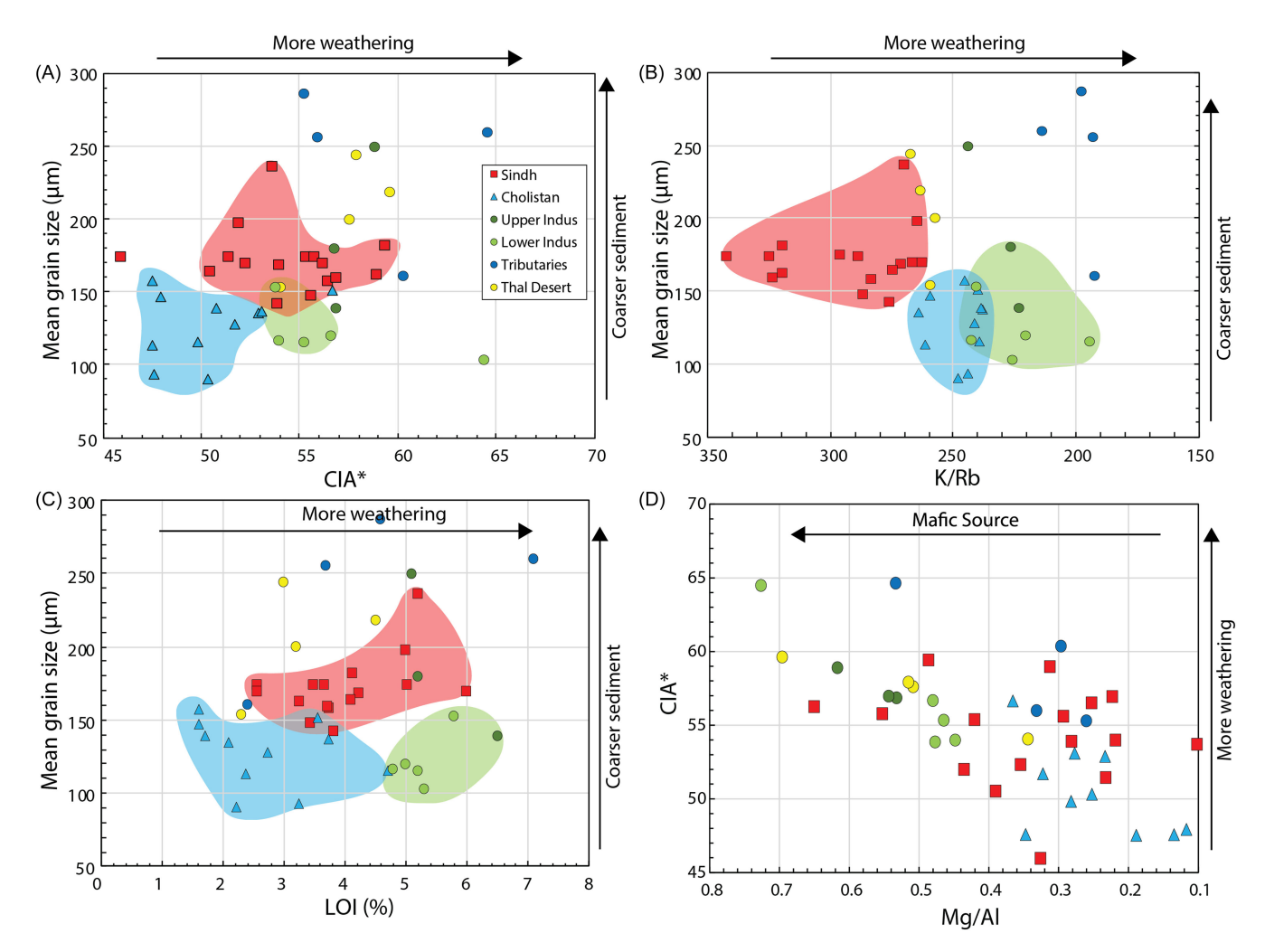


Figure 6. Cross plots, showing the relationship between mean grain size and a variety of chemical weathering indices for sediment from both the Sindh and Cholistan deserts, as well as from the Upper and Lower Indus (Garzanti et al. 2020) and major Punjabi tributaries (Clift et al. 2010b). Mean grain size versus (A) CIA\*, (B) K/Rb, (C) LOI and (D) Mg/Al.

with finer-grained sediment typically showing higher Al/Si values. The sediments show an overall coherent array between the offshore fine-grain sediments, the modern river and the Sindh and Cholistan desert sediments. This indicates that they are part of a coherent sediment grouping, but that the offshore sediments are generally finer-grained and further transported than those seen onshore in rivers and deserts. The Thal Desert and some of the mainstream Indus River depart most from this general trend. In contrast, this figure implies that marine sediment may be being reworked from the Thar Desert prior to transport offshore.

### 5.c. Mineralogical fingerprints and provenance studies

In the Indus River catchment, mafic rocks are widely exposed in the Kohistan Range and to a lesser extent in the Karakorum, both drained by the Upper Indus, whereas they are scarce in the Himalayan thrust belt drained by the Punjabi tributaries. Cholistan dune sand is feldspatho-litho-quartzose with dominant monocrystalline quartz and subequal amounts of plagioclase and K-feldspar (Usman *et al.* 2024). Sindh dune sand is litho-felspatho-quartzose, with sedimentary rock fragments prevailing over metapelite, metapsammite and metavolcanic grains. Heavy mineral assemblages in all Thar Desert sands consist of hornblende, subordinate epidote and garnet, and minor

clinopyroxene, hypersthene, staurolite, titanite, kyanite and fibrolitic sillimanite, a typical association of erosion from an orogen (Garzanti & Andò, 2007). Sindh sands have less quartz than those from Cholistan (53  $\pm$  2% vs. 60  $\pm$  2%), are more sedimentary than metamorphic lithics (Lm 39  $\pm$  6 Ls 58  $\pm$  5 vs. Lm 62  $\pm$  2 Ls 37  $\pm$  2) and have higher heavy-mineral concentrations than Cholistan sand (Usman et al. 2024). Detrital zircon U-Pb ages are dominantly Palaeozoic and Neoproterozoic, and this resembles the ages of basement rocks of the Karakorum and Himalayan sources (details in Usman et al. (2024), Section 6.2 and Figs. 6 and 7). Mesoproterozoic to Paleoproterozoic detrital zircons are primarily derived from the Greater Himalaya, Lesser Himalaya and the Nanga Parbat Massif. Younger Cretaceous to Oligocene grains are predominantly derived from the Karakorum (130-99 Ma and 43-24 Ma) and Transhimalayan arcs (96-43 Ma), whereas the Baltoro granite within the Karakorum is likely the source of Miocene grains (21–17 Ma) (Mahar et al. 2014). The combination of petrographic, heavy-mineral and detrital-geochronology methods indicates that aeolian dunes in the northern Cholistan area contain greater proportions of sediment delivered by Punjabi tributaries sourced in the Himalayan belt compared to aeolian dunes in the southern Sindh area. Southern dune sediments have a greater compositional affinity to Indus Delta sediments dated between ~7 and 14 ka, which are relatively enriched in Karakorum-Transhimalayan

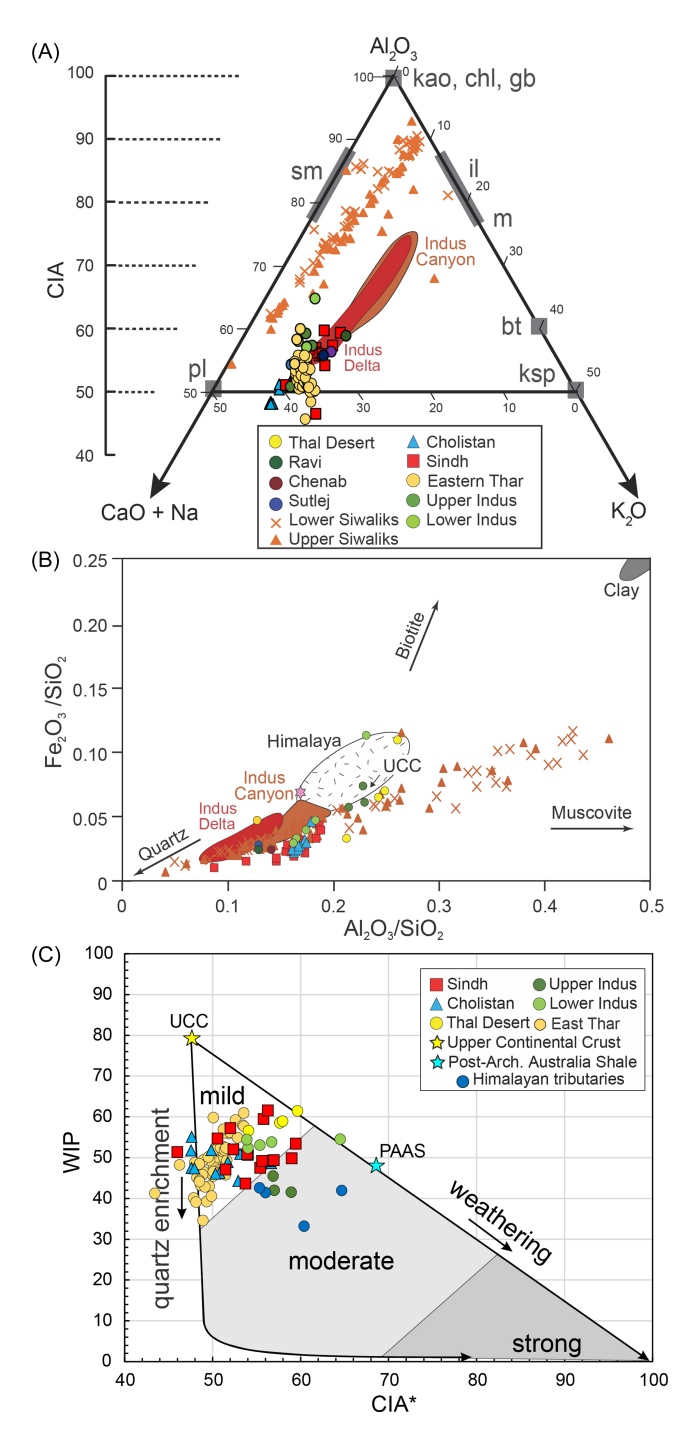


**Figure 7.** Geochemical signatures. **A)** CN-A-K ternary diagram (Fedo *et al.* 1995) comparing studied samples with the Eastern Thar Desert (Bhattacharyya *et al.* 2024), Holocene sediments from the Indus Canyon (Li *et al.* 2018) and onshore delta (Clift *et al.* 2010b). CN, A and K are the mole weights of Na<sub>2</sub>O and CaO\* (CaO associated with silicates only), Al<sub>2</sub>O<sub>3</sub> and K<sub>2</sub>O, respectively. CIA values are shown on the left side: sm, smectite; pl, plagioclase; ksp, K-feldspar; il, illite; m, muscovite. **B)** Cross plot of Fe<sub>2</sub>O<sub>3</sub>/ SiO<sub>2</sub> vs. Al<sub>2</sub>O<sub>3</sub>/SiO<sub>2</sub> used as a proxy of grain size (Singh *et al.* 2005). Data sources: Indus Canyon from Li *et al.* (2018), Indus Delta from Clift *et al.* (2010b), Siwalik Group from Vögeli *et al.* (2017) and Exnicios *et al.* (2022), and Himalaya from Galy & France-Lanord (2001). **C)** CIA\* vs. WIP plot was plotted for the Sindh and Cholistan dune sands, which are indicating slight quartz addition and less weathering intensity for the studied aeolian sands.

sediment. This could imply a higher sediment supply to the Sindh Desert in the early Holocene and more supply to the Cholistan Desert after the early Holocene when the Indus River became more Himalayan in character (Clift *et al.* 2008).

### 5.d. Sr and Nd isotope fingerprints

Sindh sand has less negative  $\epsilon_{\rm Nd}$  values not only compared to Cholistan and Eastern Thar sand but also to any sediment within the Indus River basin, apart from Thal Desert dunes (where  $\epsilon_{\rm Nd}$  values are as high as -8.7 and even -3.5) (Fig. 10a). Sindh sands are closest to the modern Upper Indus River at Tarbela Dam (Clift *et al.* 2002). The  $\epsilon_{\rm Nd}$  values of Cholistan sand, instead, largely overlap with  $\epsilon_{\rm Nd}$  values of Holocene Indus Delta sediments and with Eastern Thar sands (Bhattacharyya *et al.* 2024). Cholistan sands are slightly more  $\epsilon_{\rm Nd}$  negative than LGM sediments at the Indus River mouth (Fig. 10a). These data indicate a more primitive source for the Sindh Desert compared to Cholistan and the Eastern Thar.

The Sr and Nd isotope composition of the Indus has changed since the LGM caused by variations in erosion patterns driven by monsoon intensification (Clift *et al.* 2008). Sindh, Cholistan and Eastern Thar desert sands display  $\varepsilon_{\rm Nd}$  values less negative than Himalayan-derived sediments transported by Himalayan tributaries and deposited in the Punjab plains (Tripathi *et al.* 2004). This implies that the Thar Desert sands are mainly derived from the Indus River, in which Himalayan sources are subordinate, but these are more significant for the Cholistan and Eastern Thar Desert than in Sindh (Figs. 10a, b).

Because Sindh sand is not directly delivered from the upstream Indus but is first transported into the lower reaches, it seems most likely that Sindh received more material eroded from the exposed continental shelf and delta during the glacial era when the Indus was less  $\varepsilon_{\rm Nd}$  negative. In contrast, Cholistan and the Eastern Thar are similar to the post-glacial isotopic fingerprint. This would seem to indicate that sediments in Cholistan and the Eastern Thar Desert were transported to these locations in more recent times than those found in Sindh. However, our results imply a complete bypass of Sindh in the middle to late Holocene, although this process should not be interpreted by the source rock perspective only.

Grain size holds the key to this mismatch. Jonell et al. (2018) showed that during the Holocene, sediment >125  $\mu$ m tends to have less negative  $\varepsilon_{Nd}$  values by 1–2  $\varepsilon_{Nd}$  points than bulk sediment at the delta. The higher  $\epsilon_{\text{Nd}}$  values in Sindh are consistent with the generally coarser grain size of those samples, while the finer sediment in Cholistan has more negative  $\epsilon_{\mbox{\scriptsize Nd}}$  values. Lack of grain size information from the Eastern Thar Desert prevents testing whether the same process may be affecting the more negative  $\epsilon_{Nd}$  values there, although the longer transport distance from the delta source would favour a preponderance of finer-grained sediment in that region too. We suggest that the finer-grain sediment being supplied from the delta is transported further and preferentially deposited in the north and the eastern parts of the desert, while coarser material remains closer to the source. A simple grain size sorting by deflation could account for the observed isotopic difference. It is, however, noteworthy that even Cholistan is less  $\varepsilon_{Nd}$  negative than the post-LGM sediments and much more positive than the modern river mouth. This implies that the sediments reaching the Thar Desert were mobilized in the Early Holocene when the river had  $\epsilon_{Nd}$  values around -12, which was also a time of strong summer monsoon winds.

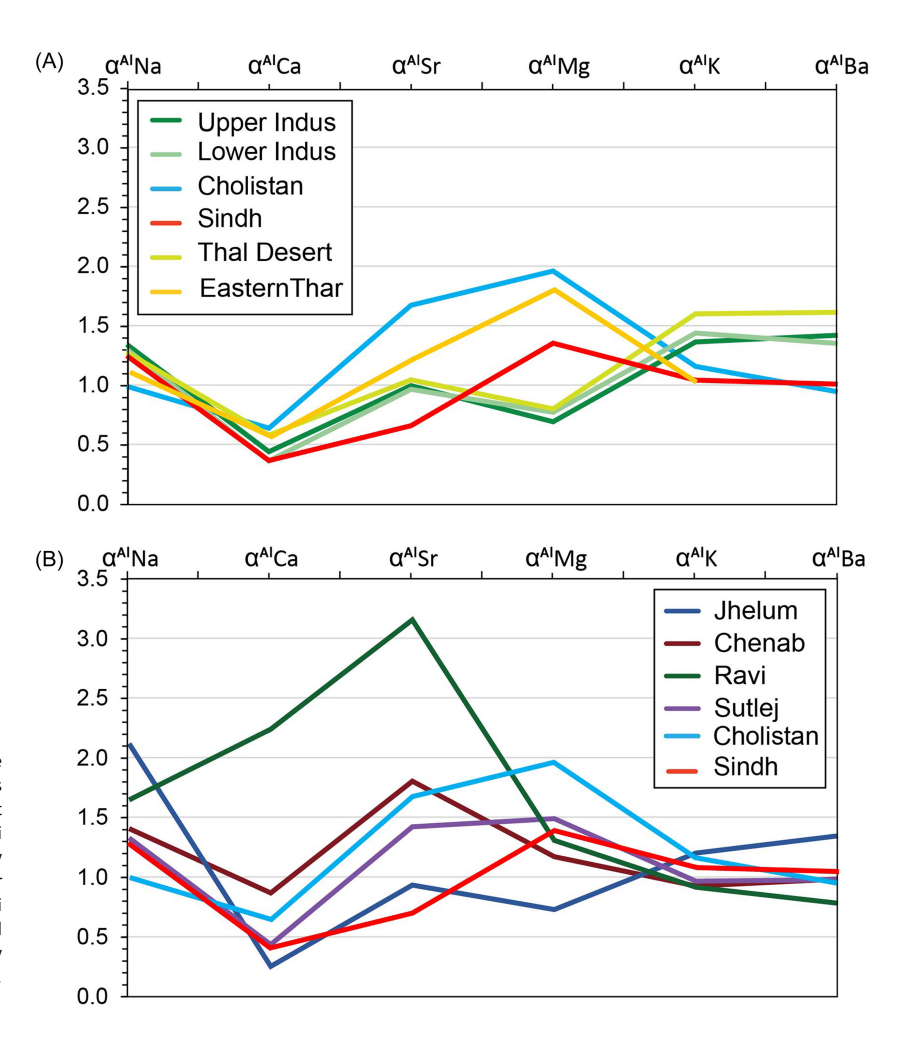


**Figure 8.** Weathering indices of Alpha<sup>Al</sup>E of sand fractions in the Thar (Sindh and Cholistan) Desert. Elemental data in previous studies were plotted for comparison, including bulk sediment (Garzanti *et al.* 2020).  $α^{Al}$  E values (Garzanti *et al.* 2014a; Garzanti *et al.* 2014b) indicate negligible weathering intensity, especially for Sindh Desert sand displaying the same fingerprint as Upper Indus, Thal Desert and Lower Indus sands (**A**, data from Garzanti *et al.* (2020)). **B**) Cholistan sand is slightly more depleted in Sr and Mg, which is an inherited effect consequence of greater supply from Himalayan Punjabi tributaries (data from Garzanti *et al.* (2020)).

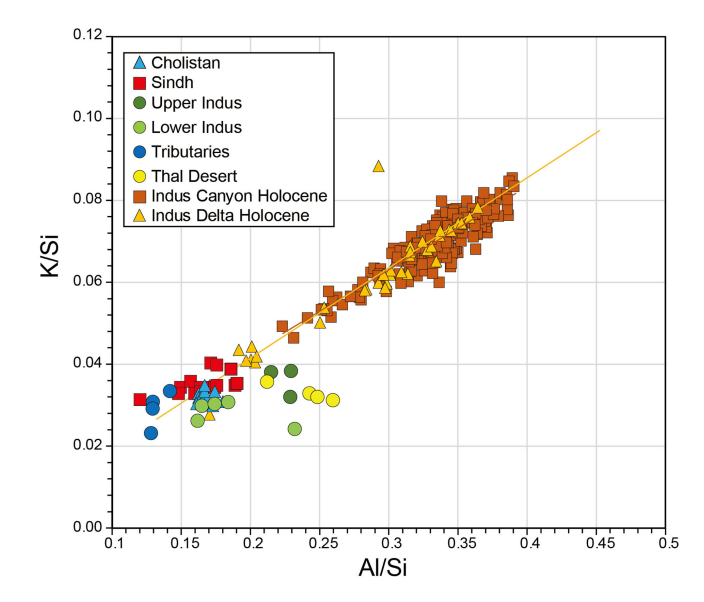


**Figure 9.** Cross plot of K/Si versus Al/Si for samples from the offshore submarine canyon and the Holocene Indus delta compared to the modern desert sands. This plot reveals differences in overall weathering intensity based on the gradient of the array (Lupker *et al.*, 2012). The gradient defined by the offshore fine-grained sediments is consistent with the desert sediments as well as the Upper and Lower Indus and the major Punjabi tributaries, indicating that they are part of a coherent sediment grouping. Canyon data are from Li *et al.* (2018). Delta data are from Clift *et al.* (2010).

# 5.e. Recycling of sand from the Indus River to the Thar Desert

The degree of recycling of sediment can be partly constrained through consideration of the 'transparent Heavy Mineral Concentration index' (tHMC) (Garzanti & Andò, 2007). This is calculated with the following equation:

$$tHMC = HMC(1 - opaque - turbid)$$

where % opaque and % turbid are the percentages of opaque and turbid heavy minerals over total heavy mineral concentration (HMC). The ZTR index is also a useful proxy and was defined by Hubert (1962) as the percentage of chemically ultra-stable species (zircon, tourmaline and rutile) among transparent detrital heavy minerals.

The low proportion of durable zircon, tourmaline and rutile (ZTR<4) argues in favour of limited recycling of older sedimentary rock detritus, which should be richer in ZTR because of the removal of less robust phases during transport or decay during diagenesis. In contrast, the high concentration of transparent heavy minerals in both regions (tHMC = 6–15%) and the common presence of pyroxene (7  $\pm$  2% of the total heavy minerals (tHM)), including both clinopyroxene and orthopyroxene), implies significant erosion from mafic rocks such as those exposed in the Kohistan and Karakorum (Liang *et al.* 2019). Himalayan tributaries carry sand with notably lower tHMC concentrations

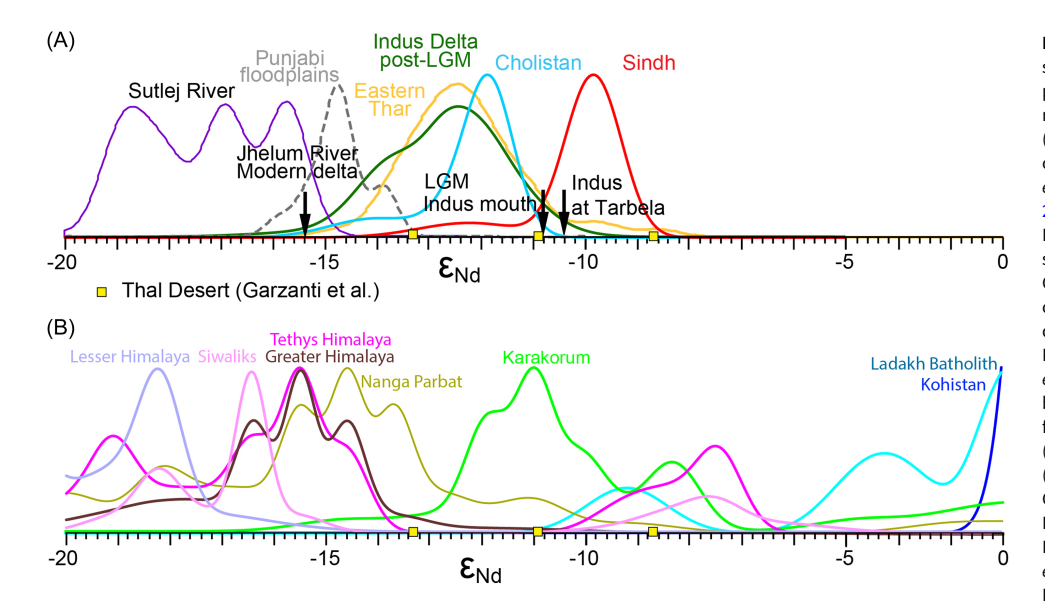


Figure 10. A) KDE plot of  $\varepsilon_{Nd}$  values of aeolian sand from Sindh and Cholistan deserts compared with sand carried by Sutlei and Jhelum rivers (Clift et al. 2002), Eastern Thar Desert (Bhattacharyya et al. 2024), Holocene sediments of Puniabi floodplain (Alizai et al. 2011a: East et al. 2015), post-LGM Indus delta (Clift et al. 2008), Upper Indus River upstream of Tarbela Dam (Garzanti et al. 2020) and river mouth/delta sediments from LGM to present (Clift et al. 2008; Clift et al. 2002). B) Range of  $\epsilon_{Nd}$  values characterizing bedrock in main geological units drained by the Indus River. Data sources: Kohistan from Petterson et al. (1993), Khan et al. (1997) & Jagoutz et al. (2019)); Ladakh batholith from Rolland et al. (2002); Karakorum from Schärer et al. (1990), Crawford & Searle (1992), Mahéo et al. (2009) and Jagoutz et al. (2019); Nanga Parbat from George et al. (1993), Gazis et al. (1998), Whittington et al. (1999), Foster (2000) and Argles et al. (2003); Tethys Himalaya from Whittington et al. (1999), Ahmad et al. (2000) and Robinson et al. (2001): Greater Himalaya from Deniel et al. (1987), Stern et al. (1989), Bouquillon et al. (1990), France-Lanord et al. (1993), Parrish & Hodges (1996), Ahmad et al. (2000), Miller et al. (2001), Robinson et al. (2001) and Martin et al. (2005); Lesser Himalaya from Bouquillon et al. (1990), Parrish & Hodges (1996), Ahmad et al. (2000) and Robinson et al. (2001); Siwaliks from Huyghe et al. (2001) and Chirouze et al. (2015).

(Sutlej = 6%, Ravi, Chenab and Beas = 1%) and with much less pyroxene (Beas = 5%, Sutlej, Ravi and Chenab = 1%) (Garzanti et al. 2020; Usman, 2024; Usman et al. 2024). Using heavy-mineral suites alone could result in underestimation of the contribution from the Himalayan tributaries, although heavy minerals may be concentrated by hydrodynamic sorting.

Thermoluminescence dating of aeolian sediments from the Thar Desert has revealed multiple phases of dune accretion, sand recycling and accumulation that may have taken place in the last 200 k.y. (Nitundil et al. 2023; Singhvi et al. 2010). Zircon grains with U-Pb diagnostic signatures of Upper Indus provenance (i.e., 43-96 Ma for Transhimalayan arcs and 130-99 Ma, 43-24 Ma and 21-17 Ma for Karakorum and Baltoro Granite) occur both in Sindh and Cholistan sands but not in Himalayan-derived sand carried by the eastern tributaries draining the edges of the Cholistan Desert. This suggests that Indus sand has been extensively blown northward, especially in the Sindh Desert, by wind transportation during the latest glacial-interglacial cycles (Usman et al. 2024). Sand transported by the eastern Himalayan tributaries tends to exhibit depletion in most elements compared to the UCC (this study and Garzanti et al. (2020)), which indicates much more extensive recycling from sedimentary and metasedimentary rocks (Figs. 4b, 8 and S2).

Garzanti *et al.* (2020) further noted that Lower Indus sand is depleted in most elements except Si, Ca and P when contrasted with Upper Indus sand. This points to a significant additional contribution from erosion of quartz-rich metasedimentary and siliciclastic rocks. Enhanced reworking by river incision of older floodplain sediments occurred during the Holocene (Giosan *et al.* 2012), as well as after the onset of extensive agricultural activities (Li *et al.* 2019). Furthermore, relative to the Lower Indus River sand, deltaic sediments from the LGM to the Holocene period and Thar Desert sediments display enrichment in most elements (Fig. S2).

# 5.f. Comparative provenance signatures of the Thar Desert and sources

The two distinct provenance patterns of the Thar Desert sands are relative to potential sources in the Upper and Lower Indus, in the Punjab tributaries and the Indus Delta, as shown in the conceptual Figure 11 and Table 4. The Sindh Desert sands are coarser, have lower SiO<sub>2</sub>, higher CaO, Sr-Cr-Nb enrichment and less negative  $\varepsilon_{Nd}$  values (-9 to -12), which closely resemble Indus Delta and Upper Indus sediments derived from Karakorum and Transhimalayan arcs. Sands of the Cholistan Desert are finer and more quartz- and  $Al_2O_3$ -enriched, have lower  $\varepsilon_{Nd}$  values (-12 to -14) and greater proportions of metamorphic lithics and Proterozoic zircon populations, suggesting more Greater and Lesser Himalayan sources via Punjab tributaries. Upper Indus sands are more mafic-enriched, while Punjab tributaries deliver more Al<sub>2</sub>O<sub>3</sub>, transition metals and Proterozoic zircons, with Indus Delta deposits having a composite signal as might be expected. In general, the Thar Desert records a bimodal provenance pattern: southern Sindh is linked to Indus/Transhimalayan sources, and northern Cholistan is linked to Himalayan Punjabi tributary sources.

## 6. Conclusions

This study compares elemental geochemistry, isotope geochemistry and mineralogical and geochronological signatures of aeolian sand in the Sindh and Cholistan regions of the western Thar Desert. Closer affinity to sediment carried during the Early Holocene by the Indus River compared to by its major Himalayan tributaries helped us to determine the provenance of the dune sand and to investigate the processes leading to the growth of the Thar Desert through geological time. Elemental and isotope geochemistry are consistent with petrographic and mineralogical

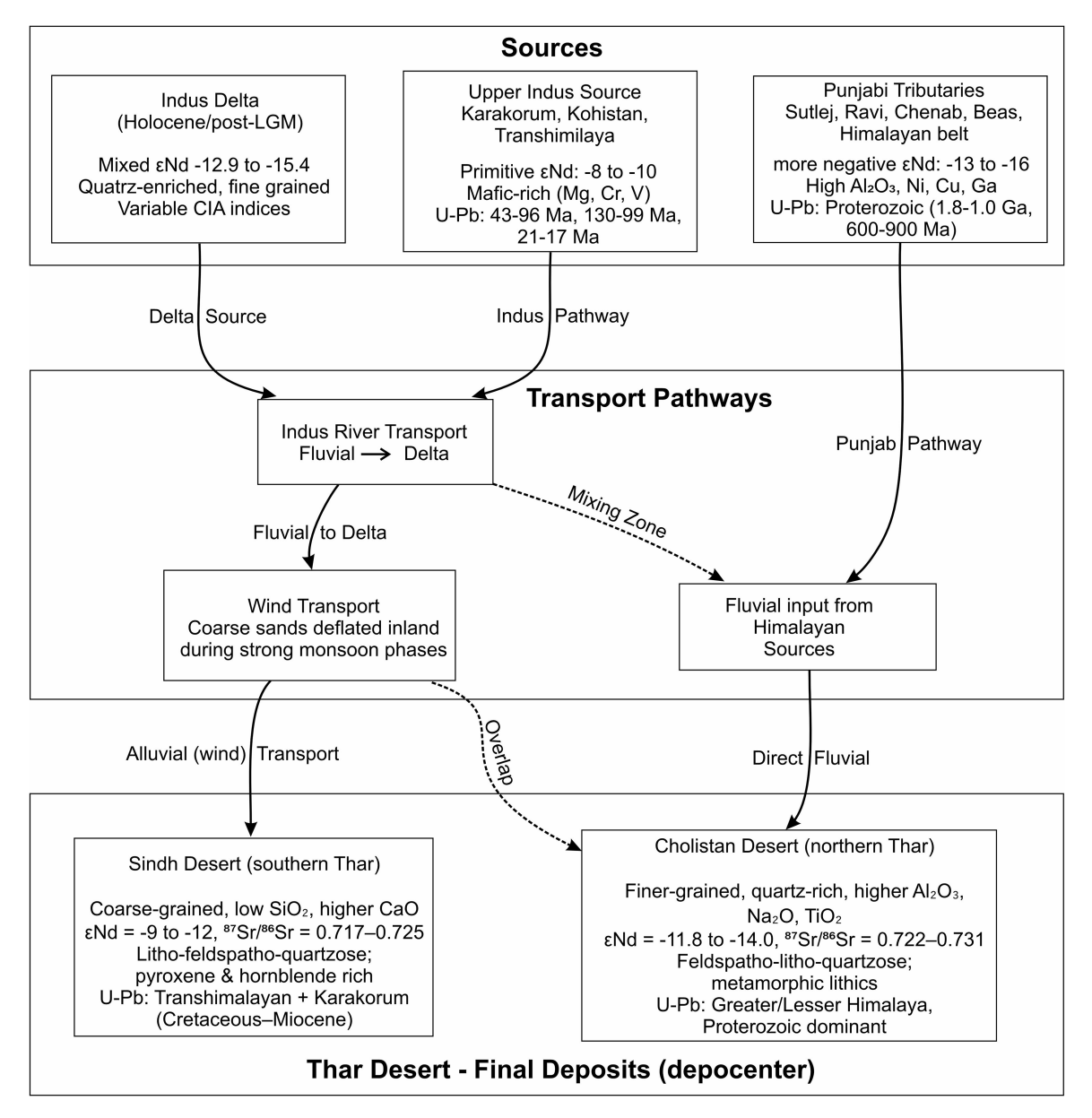


**Figure. 11.** This conceptual diagram visually explains the provenance and transport history of sand in the Thar Desert, demonstrating why the southern Sindh Desert and the northern Cholistan Desert sand have different compositions.

evidence in indicating that sand in the southern Sindh region is largely derived from deflation of the Indus River floodplain and delta, especially during the post-LGM period. Sand in the northern Cholistan region shows greater compositional similarity with Himalayan tributaries. Although this would imply delivery of sediment during the mid-late Holocene as the river evolved to more Himalayan compositions, this is inconsistent with the longer distance between the delta and the desert in Cholistan. The less negative  $\epsilon_{\rm Nd}$  values in Sindh compared to Cholistan or the modern river mouth require preferential supply from primitive sources.

The early post-LGM delta has the closest match in  $\epsilon_{Nd}$  values to sands in Cholistan, but this may simply reflect the fact that the sediment is coarser, indicating a grain-size control biased in favour of Karakorum sources (Jonell *et al.* 2018). The compositional differences between the south and the north can therefore be understood as reflecting deflation of coarser sediment in the south and the concentration of finer Himalaya sediments in the north. This

assessment is confirmed by the higher concentration of elements such as Mg and Cr preferentially hosted in mafic rocks, implying that a larger proportion of Sindh sand is supplied from erosion of mafic rocks in the Upper Indus River catchment. Mafic source rocks are widely exposed in these regions, especially in the Kohistan and Karakorum, but are scarce in the Himalayan Belt drained by Punjabi tributaries. The dominant supply from the post-LGM lower Indus River to the Thar Desert suggests that most aeolian sediment transport is linked to southwesterly summer monsoon winds blowing from the delta region inland in recent times.

**Supplementary material.** The supplementary material for this article can be found at https://doi.org/10.1017/S0016756825100320.

**Acknowledgements.** MU would like to thank the PhD programme of the Department of Earth and Environmental Sciences, University of Milano-Bicocca, Italy, for supporting his research and the International Union for Quaternary Research (INQUA) for receiving a research grant as an Early Career

Scientist. PC thanks the Charles T. McCord Jr chair in petroleum geology at LSU for support during this work. We are also thankful to Dr Saif Ur Rehman for help during fieldwork. This article is an outcome of project MIUR – Dipartimenti di Eccellenza 2023–2027, Department of Earth and Environmental Sciences, University of Milano-Bicocca, Italy.

#### References

- Ahmad F (2008) Runoff farming in reducing rural poverty in Cholistan desert. Sociedade & Natureza 20, 177–88.
- Ahmad T, Harris N, Bickle M, Chapman H, Bunbury J and Prince C (2000) Isotopic constraints on the structural relationships between the Lesser Himalayan Series and the High Himalayan Crystalline Series, Garhwal Himalaya. *Geological Society of America Bulletin* 112(3), 467–77.
- Alizai A, Carter A, Clift PD, VanLaningham S, Williams JC and Kumar R (2011a) Sediment provenance, reworking and transport processes in the Indus River by U-Pb dating of detrital zircon grains. Global and Planetary Change 76 33–55, doi: 10.1016/j.gloplacha.2010.11.008.
- Alizai A, Clift PD, Giosan L, VanLaningham S, Hinton R, Tabrez AR, Danish M. and EIMF (2011b) Pb Isotopic Variability in the Modern and Holocene Indus River System measured by Ion Microprobe in detrital K-feldspar grains. *Geochimica et Cosmochimica Acta* 75, 4771–95, doi: 10.1016/j.gca.2011.05.039.
- Allen PA (2008) Time scales of tectonic landscapes and their sediment routing systems. Geological Society, London, Special Publications 296(1), 7–28, doi: 10.1144/SP296.2.
- Argles T, Foster G, Whittington A, Harris N and George M (2003) Isotope studies reveal a complete Himalayan section in the Nanga Parbat syntaxis. Geology 31(12), 1109–12.
- Bhattacharyya R, Singh SP, Qasim A and Chandrashekhar AK (2024)
  Geochemical and Radiogenic Sr-Nd Isotope Characterization of Widespread
  Sandy Surface Sediments in the Great Indian Desert, Thar: Implications for
  Provenance Studies. *Journal of Geophysical Research: Earth Surface* 129(8),
  e2023JF007625, doi: 10.1029/2023JF007625.
- Bloemsma MR, Zabel M, Stuut JBW, Tjallingii R, Collins JA and Weltje GJ (2012) Modelling the joint variability of grain size and chemical composition in sediments. *Sedimentary Geology* **280**, 135–148. doi: 10.1016/j.sedgeo.2012. 04.009.
- **Blum MD and Törnqvist TE** (2000) Fluvial responses to climate and sea-level change: a review and look forward. *Sedimentology* **47**, 2–48.
- Bookhagen B and Burbank DW (2006) Topography, relief, and TRMM-derived rainfall variations along the Himalaya. *Geophysical Research Letters* 33(8), doi: 10.1029/2006GL026037.
- Bookhagen B. and Burbank DW (2010) Towards a complete Himalayan hydrological budget: The spatiotemporal distribution of snow melt and rainfall and their impact on river discharge. *Journal of Geophysical Research* 115(F3), doi: 10.1029/2009jf001426.
- Bostock HC, Opdyke BN, Gagan MK, Kiss AE and Fifield LK (2006) Glacial/ interglacial changes in the East Australian current. *Climate Dynamics* **26**(6), 645–59, doi: 10.1007/s00382-005-0103-7.
- Bouquillon A, France-Lanord C, Michard A. and Tiercelin J. (1990)
  Sedimentology and isotopic chemistry of the Bengal Fan sediments: the denudation of the Himalaya. In *Proceedings of the Ocean Drilling Program, Scientific Results* (eds JR Cochran, DAV Stow and C Auroux), pp. 43–58.
  College Station, TX: Ocean Drilling Program. 116, doi: 10.2973/odp.proc.sr. 116.117.1990.
- Burbank DW, Blythe AE, Putkonen J, Pratt-Sitaula B, Gabet E, Oskins M, Barros A and Ojha TP (2003) Decoupling of erosion and precipitation in the Himalayas. *Nature* **426**, 652–55.
- Chirouze F, Huyghe P, Chauvel C, van der Beek P, Bernet M and Mugnier J-L (2015) Stable Drainage Pattern and Variable Exhumation in the Western Himalaya since the Middle Miocene. *Journal of Geology* **123**, 1–20, doi: 10. 1086/679305.
- Clift PD, Campbell IH, Pringle MS, Carter A, Zhang X, Hodges KV, Khan AA and Allen CM (2004) Thermochronology of the modern Indus River bedload; new insight into the control on the marine stratigraphic record. *Tectonics* 23(5), doi: 10.1029/2003TC001559.

- Clift PD, Carter A, Giosan L., Durcan J, Tabrez AR, Alizai A, Van Laningham S, Duller GAT, Macklin MG, Fuller DQ and Danish M (2012) U-Pb zircon dating evidence for a Pleistocene Sarasvati River and Capture of the Yamuna River. *Geology* 40(3), 212–15, doi: 10.1130/G32840.1.
- Clift PD and Giosan L (2014) Sediment fluxes and buffering in the post-glacial Indus Basin. Basin Research 26, 369–86, doi: 10.1111/bre.12038.
- Clift PD, Giosan L, Blusztajn J, Campbell IH, Allen CM, Pringle M, Tabrez A, Danish M, Rabbani MM, Carter A and Lückge A (2008) Holocene erosion of the Lesser Himalaya triggered by intensified summer monsoon. *Geology* **36**(1), 79–82, doi: 10.1130/G24315A.1.
- Clift PD, Giosan L, Carter A, Garzanti E, Galy V, Tabrez AR, Pringle M, Campbell IH, France-Lanord C, Blusztajn J, Allen C, Alizai A, Lückge A, Danish M and Rabbani MM (2010a) Monsoon control over erosion patterns in the Western Himalaya: possible feed-backs into the tectonic evolution. In *Monsoon Evolution and Tectonic-Climate Linkage in Asia* (eds P. D. Clift, R. Tada and H. Zheng), pp. 181–213. London: Geological Society. Special Publication, 342, .
- Clift PD and Jonell TN (2021) Monsoon controls on sediment generation and transport: Mass budget and provenance constraints from the Indus River catchment, delta and submarine fan over tectonic and multi-millennial timescales. Earth-Science Reviews 220, 103682, doi: 10.1016/j.earscirev.2021. 103682.
- Clift PD, Lee JI, Hildebrand P, Shimizu N, Layne GD, Blusztajn J, Blum J D, Garzanti E and Khan AA (2002) Nd and Pb isotope variability in the Indus River system; implications for sediment provenance and crustal heterogeneity in the western Himalaya. *Earth and Planetary Science Letters* **200**(1-2), 91–106, doi: 10.1016/S0012-821X(02)00620-9.
- Clift PD and Plumb RA (2008) The Asian Monsoon: Causes, History and Effects. Cambridge: Cambridge University Press.
- Clift PD, Tada R and Zheng H, (eds.) (2010b) Monsoon Evolution and Tectonic-Climate Linkage in Asia. London: Geological Society.
- Colin C, Siani G, Sicre M-A and Liu Z (2010) Impact of the East Asian monsoon rainfall changes on the erosion of the Mekong River basin over the past 25,000 yr. *Marine Geology* 271(1-2), 84–92, doi: 10.1016/j.margeo.2010. 01.013.
- Crawford MB and Searle MP (1992) Field relationships and geochemistry of pre-collisional (India-Asia) granitoid magmatism in the central Karakoram, northern Pakistan. *Tectonophysics* **206**, 171–92.
- Cronin TM 1999. Principles of Paleoclimatology. Columbia University Press. Deniel C, Vidal P, Fernandez A, Lefort P and Peucat JJ (1987) Isotopic Study of the Manaslu Granite (Himalaya, Nepal) Inferences on the Age and Source of Himalayan Leukogranites. Contributions to Mineralogy and Petrology 96(1), 78–92.
- Dhir RP, Singhvi AK, Andrews JE, Kar A, Sareen BK, Tandon SK, Kailath A and Thomas JV (2010) Multiple episodes of aggradation and calcrete formation in Late Quaternary aeolian sands, Central Thar Desert, Rajasthan, India. *Journal of Asian Earth Sciences* 37, 10–16, doi: 10.1016/j.jseaes.2009.07.002.
- Dinis P, Garzanti E, Vermeesch P and Huvi J (2017) Climatic zonation and weathering control on sediment composition (Angola). *Chemical Geology* **467**, 110–21, doi: 10.1016/j.chemgeo.2017.07.030.
- Duzgoren-Aydin NS and Aydin A (2003) Chemical Heterogeneities of Weathered Igneous Profiles: Implications for Chemical Indices. Environmental & Engineering Geoscience 9(4), 363–76, 10.2113/9.4.363.
- East AE, Clift PD, Carter A, Alizai A and VanLaningham S (2015) Fluvial– Eolian Interactions In Sediment Routing and Sedimentary Signal Buffering: An Example From the Indus Basin and Thar Desert. *Journal of Sedimentary Research* 85, 715–28, doi: 10.2110/jsr.2015.42.
- Exnicios EM, Carter A, Najman Y and Clift PD (2022) Late Miocene unroofing of the Inner Lesser Himalaya recorded in the NW Himalaya foreland basin. *Basin Research* **34**(6), 1894–916, doi: 10.1111/bre.12689.
- Fedo CM, Nesbitt HW and Young GM (1995) Unraveling the effects of potassium metasomatism in sedimentary rocks and paleosols, with implications for paleoweathering conditions and provenance. Geology 23, 921–24.
- Fildani A, McKay MP, Stockli D, Clark J, Dykstra ML, Stockli L and Hessler AM (2016) The ancestral Mississippi drainage archived in the late Wisconsin Mississippi deep-sea fan. Geology 44, 479–82. 10.1130/g37657.1.

- Folk RL and Ward WC (1957) Brazos River bar [Texas]; a study in the significance of grain size parameters. *Journal of Sedimentary Research* 27(1), 3–26, doi: 10.1306/74d70646-2b21-11d7-8648000102c1865d.
- **Foster GL** (2000) The pre-Neogene thermal history of the Nanga Parbat Haramosh Massif and the NW Himalaya. The Open University.
- France-Lanord C, Derry L and Michard A (1993) Evolution of the Himalaya since Miocene time: Isotopic and sedimentologic evidence from the Bengal Fan. In *Himalayan Tectonics* (eds PJ Treloar and MP Searle), pp. 603–21. London: Geological Society. Special Publications, 74.
- Gabet, E. J. and Mudd S. M. (2009) A theoretical model coupling chemical weathering rates with denudation rates. *Geology* 37(2), 151–54, doi: 10.1130/g25270a.1.
- Gaillardet J, Dupré B and Allègre CJ (1999) Geochemistry of large river suspended sediments: silicate weathering or recycling tracer? Geochimica et Cosmochimica Acta 63(23-24), 4037–51.
- **Galewsky J** (2009) Rain shadow development during the growth of mountain ranges: An atmospheric dynamics perspective. *Journal of Geophysical Research: Earth Surface* **114**(F1), doi: 10.1029/2008JF001085.
- Galy A and France-Lanord C (2001) Higher erosion rates in the Himalaya: Geochemical constraints on riverine fluxes. Geology 29(1), 23–26.
- Garzanti E and Andò S (2007) Heavy-mineral concentration in modern sands: implications for provenance interpretation. In *Heavy Minerals in Use* (eds M. Mange and D. Wright), pp. 517–45. Amsterdam: Elsevier. Developments in Sedimentology Series, 58.
- Garzanti E, Liang W, Andò S, Clift PD, Resentini A, Vermeesch P and Vezzoli G (2020) Provenance of Thal Desert sand: focused erosion in the western Himalayan syntaxis and foreland-basin deposition driven by latest Quaternary climate change. *Earth-Science Reviews* 207, 103220, doi: 10.1016/j.earscirev.2020.103220.
- Garzanti E, Padoan M, Andò S, Resentini A, Vezzoli G and Lustrino M (2013a) Weathering and relative durability of detrital minerals in equatorial climate: sand petrology and geochemistry in the East African Rift. *The Journal of Geology* 121(6), 547–80, doi: 10.1086/673259.
- Garzanti E, Padoan M, Setti M, López-Galindo A and Villa IM (2014a) Provenance versus weathering control on the composition of tropical river mud (southern Africa). Chemical Geology 366, 61–74, doi: 10.1016/j.che mgeo.2013.12.016.
- Garzanti E, Padoan M, Setti M, Najman Y, Peruta L and Villa IM (2013b) Weathering geochemistry and Sr-Nd fingerprints of equatorial upper Nile and Congo muds. *Geochemistry, Geophysics, Geosystems* **14**(2), 292–316, doi: 10.1002/ggge.20060.
- Garzanti E, Pastore G, Stone A, Vainer S, Vermeesch P and Resentini A (2022) Provenance of Kalahari Sand: Paleoweathering and recycling in a linked fluvial-aeolian system. *Earth-Science Reviews* 224, 103867, doi: 10.1016/j.earscirev.2021.103867.
- Garzanti E and Resentini A (2016) Provenance control on chemical indices of weathering (Taiwan river sands). Sedimentary Geology 336, 81–95, doi: 10.1016/j.sedgeo.2015.06.013.
- Garzanti E, Vermeesch P, Padoan M, Resentini A, Vezzoli G and Ando S (2014b) Provenance of Passive-Margin Sand (Southern Africa). *The Journal of Geology* **122**(1), 17–42, doi: 10.1086/674803.
- Garzanti E, Vezzoli G, Ando S, Paparella P and Clift PD (2005) Petrology of Indus River sands; a key to interpret erosion history of the western Himalayan syntaxis. *Earth and Planetary Science Letters* **229**(3-4), 287–302, doi: 10.1016/j.epsl.2004.11.008.
- Gazis C, Blum J, Chamberlain C and Poage M (1998) An isotopic study of granite genesis: Nanga-Parbat Haramosh Massif. Pakistan Himalaya: American Journal of Science 298, 673–98.
- Gebregiorgis D, Hathorne EC, Sijinkumar AV, Nath BN, Nürnberg D and Frank M (2016) South Asian summer monsoon variability during the last ~54 kyrs inferred from surface water salinity and river runoff proxies. *Quaternary Science Reviews* 138, 6–15, doi: 10.1016/j.quascirev.2016.02.012.
- George MT, Harris NBW and Butler RWH (1993) The tectonic implications of contrasting granite magmatism between the Kohistan island arc and the Nanga Parbat-Haramosh Massif, Pakistan Himalaya. Geological Society, London, Special Publications 74(1), 173–91, doi: 10.1144/GSL.SP.1993.074. 01.13.

- Giosan L., Clift P. D., Macklin M. G., Fuller D. Q., Constantinescu S., Durcan J. A., Stevens T., Duller G. A. T., Tabrez A., Adhikari R., Gangal K., Alizai A., Filip F., VanLaningham S and Syvitski JPM (2012) Fluvial Landscapes of the Harappan Civilization. *Proceedings Of The National Academy of Sciences* 109(26), 1688–94, doi: 10.1073/pnas.1112743109.
- Glennie KW and Singhvi A (2002) Event stratigraphy, paleoenviron- ment and chronology of SE Arabian deserts. Quaternary Science Reviews 21, 853–69.
- Glennie KW, Singhvi AK, Lancaster N and Teller JT (2002) Quaternary climatic changes over Southern Arabia and the Thar Desert, India. In *The Tectonic and Climatic Evolution of the Arabian Sea Region* (eds PD Clift, D Kroon, C Gaedicke and J Craig), pp. 301–16. London: Geological Society. Special Publications, 195, doi: 10.1144/GSL.SP.2002.195.01.16.
- Goldstein SL, O'Nions RK and Hamilton PJ (1984) A Sm-Nd isotopic study of atmospheric dusts and particulates from major river systems. *Earth and Planetary Science Letters* **70**(2), 221–36.
- Guo Y, Yang S and Deng K (2021) Disentangle the hydrodynamic sorting and lithology effects on sediment weathering signals. *Chemical Geology* 586, 120607. doi: 10.1016/j.chemgeo.2021.120607.
- Herman F and Champagnac J-D (2016) Plio-Pleistocene increase of erosion rates in mountain belts in response to climate change. *Terra Nova* 28(1), 2–10, doi: 10.1111/ter.12186.
- Hu D, Clift PD, Wan S, Böning P, Hannigan R, Hillier S and Blusztajn J (2016) Testing chemical weathering proxies in Miocene–Recent fluvial-derived sediments in the South China Sea. In *River-Dominated Shelf Sediments of East Asian Seas* (eds PD Clift, J Harff, J Wu and Y Qiu). London: Geological Society. Special Publication, 429, doi: 10.1144/SP429.5.
- Hubert JF (1962) A zircon-tourmaline-rutile maturity index and the interdependence of the composition of heavy mineral assemblages with the gross composition and texture of sandstones. *Journal of Sedimentary Research* 32(3), 440–50, doi: 10.1306/74d70ce5-2b21-11d7-8648000102c1865d.
- Huntington KW, Blythe AE and Hodges KV (2006) Climate change and late Pliocene acceleration of erosion in the Himalaya. Earth and Planetary Science Letters 252(1-2), 107–18.
- Huyghe P, Galy A, Mugnier J-L and France-Lanord C (2001) Propagation of the thrust system and erosion in the Lesser Himalaya: Geochemical and sedimentological evidence. *Geology* **29**(11), 1007–10.
- Inam A, Clift PD, Giosan L, Tabrez AR, Tahir M, Rabbani MM and Danish M (2007) The geographic, geological and oceanographic setting of the Indus River. In *Large Rivers: Geomorphology and Management* (ed A. Gupta), pp. 333–45. Chichester, UK: John Wiley and Sons.
- Jagoutz O. Bouilhol P. Schaltegger U. and Müntener O (2019) The isotopic evolution of the Kohistan Ladakh arc from subduction initiation to continent arc collision. *Geological Society, London, Special Publications* 483(1), 165–82, doi: 10.1144/SP483.7.
- Jonell T. N., Li Y., Blusztajn J, Giosan L and Clift PD (2018) Signal or noise? Isolating grain size effects on Nd and Sr isotope variability in Indus delta sediment provenance. *Chemical Geology* 485, 56–73, doi: 10.1016/j.chemgeo. 2018.03.036.
- Kar A, Felix C, Rajaguru S. N. and Singhvi A. K. (1998) Late Holocene growth and mobility of a transverse dune in the Thar Desert. *Journal of Arid Environments* 38(2), 175–85, DOI: 10.1006/jare.1997.0343.
- Khan I, Sinha R, Murray AS and Jain M (2024) Landscape evolution of the NW Himalayan rivers during the late Quaternary and their non-contemporaneity to the Harappan Civilization. *Quaternary Science Reviews* 331, 108622, doi: 10.1016/j.quascirev.2024.108622.
- Khan MA, Stern RJ, Gribble RF and Windley BF (1997) Geochemical and isotopic constraints on subduction polarity, magma sources, and palaeogeography of the Kohistan intra-oceanic arc, northern Pakistan Himalaya. *Journal of the Geological Society, London* 154, 935–46.
- Kuehl SA, Alexander CR, Blair NE, Harris CK, Marsaglia KM, Ogston AS, Orpin AR, Roering JJ, Bever AJ, Bilderback EL, Carter L, Cerovski-Darriau C, Childress LB, Reide Corbett D, Hale RP, Leithold EL, Litchfield N, Moriarty JM, Page MJ, Pierce LER, Upton P and Walsh JP (2016) A source-to-sink perspective of the Waipaoa River margin. *Earth-Science Reviews* 153, 301–34, doi: 10.1016/j.earscirev.2015.10.001.
- Kump LR, Brantley SL and Arthur MA (2000) Chemical weathering, atmospheric CO2, and climate. *Annual Review of Earth and Planetary Sciences* 28, 611–67.

- Li Y, Clift PD, Böning P, Blusztajn J, Murray RW, Ireland T, Pahnke K, Helm NC and Giosan L (2018) Continuous Holocene input of river sediment to the Indus Submarine Canyon. *Marine Geology* 406, 159–76, doi: 10.1016/j.margeo.2018.09.011.
- Li Y, Clift PD Murray RW Exnicios E Ireland T and Böning P (2019) Asian Summer Monsoon Influence on Chemical Weathering and Sediment Provenance determined by Clay Mineral Analysis from the Indus Submarine Canyon. *Quaternary Research* 93, 23–39. doi: 10.1017/qua.2019.44.
- Liang W, Garzanti E, Andò S, Gentile P and Resentini A (2019) Multimineral Fingerprinting of Transhimalayan and Himalayan Sources of Indus-Derived Thal Desert Sand (Central Pakistan). *Minerals* 9(8), 457.
- Lupker M, France-Lanord C, Galy V, Lave J, Gaillardet J, Gajured AP, Guilmette C,Rahman M, Singh SK and Sinha R (2012) Predominant floodplain over mountain weathering of Himalayan sediments (Ganga basin). Geochimica et Cosmochimica Acta 84, 410–32.
- Mahar MA, Mahéo G, Goodell PC and Pavlis TL (2014) Age and origin of post collision Baltoro granites, south Karakoram, North Pakistan: Insights from in-situ U-Pb, Hf and oxygen isotopic record of zircons *Lithos* 205, 341–58
- Mahéo G, Blichert-Toft J, Pin C, Guillot S and Pêcher A (2009) Partial Melting of Mantle and Crustal Sources beneath South Karakorum, Pakistan: Implications for the Miocene Geodynamic Evolution of the India–Asia Convergence Zone. *Journal of Petrology* 50(3), 427–49, doi: 10.1093/petrology/egp006.
- Martin AJ, DeCelles PG, Gehrels GE, Patchett PJ and Isachsen C (2005) Isotopic and structural constraints on the location of the Main Central Thrust in the Annapurna Range, central Nepal Himalaya. *Geological Society of America Bulletin* 117(7-8), 926–44.
- Maslov AV and Podkovyrov VN (2023) Intensity of Chemical Weathering in the Late Precambrian: New Data on the Riphean Stratotype, South Urals. Stratigraphy and Geological Correlation 31(1), 1–16, doi: 10.1134/ \$0869593823020065.
- Mason CC, Romans BW, Stockli DF, Mapes RW and Fildani A (2019)
  Detrital zircons reveal sea-level and hydroclimate controls on Amazon River to deep-sea fan sediment transfer. *Geology* 47(6), 563–67, doi: 10.1130/g45852.1.
- McLennan SM (1993) Weathering and global denudation. The Journal of Geology 101, 295–303.
- Mehdi SM, Pant NC, Saini HS, Mujtaba SAI and Pande P (2016) Identification of palaeochannel configuration in the Saraswati River basin in parts of Haryana and Rajasthan, India, through digital remote sensing and GIS. *Episodes* **39**, 29–38, doi: 10.18814/epiiugs/2016/v39i1/89234.
- Miller C, Thöni M, Frank W, Grasemann B, Klotzli U, Guntli P and Draganits E (2001) The early Paleozoic magmatic event in the northwest Himalaya, India: source, tectonic setting and age of emplacement. Geological Magazine 138, 237–51.
- Milliman JD and Farnsworth KL (2011) River Discharge to the Coastal Ocean: A Global Synthesis p. 384. Cambridge, UK: Cambridge University Press. doi: 10.1017/CBO9780511781247.
- Minyuk PS, Borkhodoev VY and Wennrich V (2014) Inorganic geochemistry data from Lake El'gygytgyn sediments: marine isotope stages 6–11. *Climate of the Past* 10(2), 467–85, doi: 10.5194/cp-10-467-2014.
- Nesbitt HW, Fedo CM and Young GM (1997) Quartz and feldspar stability, steady and non-steady-state weathering, and petrogenesis of siliciclastic sands and muds. *Journal of Geology* 105(2), 173–91.
- Nesbitt HW, Markovics G and Price RC (1980) Chemical processes affecting alkalis and alkaline earths during continental weathering. *Geochimica et Cosmochimica Acta* 44, 1659–66.
- Nesbitt HW. and Young G. M. (1982) Early Proterozoic climates and plate motions inferred from major element chemistry of lutites. *Nature* 299(5885), 715–17.
- Nesbitt HW and Young GM (1989) Formation and diagenesis of weathering profiles. *Journal of Geology* **97**(2), 129–47.
- Neubeck N, Carter A, Rittenour T and Clift PD (2023) Climate and anthropogenic impacts on North American erosion and sediment transport since the Last Glacial Maximum: Evidence from the detrital zircon record of the Lower Mississippi Valley, USA. GSA Bulletin 135, 2648–63, doi: 10.1130/ b36565.1.

- Nitundil S, Stone A and Srivastava A (2023) Applicability of using portable luminescence reader for rapid age-assessments of dune accumulation in the Thar desert, India. *Quaternary Geochronology* 78, 101468, doi: 10.1016/j.qua geo.2023.101468.
- Parker A (1970) An index of weathering for silicate rocks. Geological Magazine 107, 501–04.
- Parrish RR and Hodges KV (1996) Isotopic constraints on the age and provenance of the Lesser and Greater Himalayan sequences, Nepalese Himalaya. Geological Society of America Bulletin 108(7), 904–11.
- Petterson MG, Crawford MB and Windley BF (1993) Petrogenetic implications of neodymium isotope data from the Kohistan batholith, North Pakistan. *Journal of the Geological Society* **150**(1), 125–29, doi: 10. 1144/gsjgs.150.1.0125.
- Price DG (1995) Weathering and weathering processes. Quarterly Journal of Engineering Geology and Hydrogeology 28(3), 243–52, doi: 10.1144/gsl.Qje gh.1995.028.P3.03.
- Price JR and Velbel MA (2003) Chemical weathering indices applied to weathering profiles developed on heterogeneous felsic metamorphic parent rocks. Chemical Geology 202, 397–416.
- Reiners PW, Ehlers TA, Mitchell SG and Montgomery DR (2003) Coupled spatial variations in precipitation and long-term erosion rates across the Washington Cascades. *Nature* 426(6967), 645–47.
- Riebe CS, Kirchner JW and Finkel RC (2004) Erosional and climatic effects in long- term chemical weathering rates in granitic landscapes spanning diverse climate regimes. Earth and Planetary Science Letters 224, 547–62.
- Robinson, DM, DeCelles PG, Patchett PJ and Garzione CN (2001) The kinematic evolution of the Nepalese Himalaya interpreted from Nd isotopes. *Earth and Planetary Science Letters* **192**(4), 507–21.
- Rolland Y, Picard C, Pecher A, Lapierre H, Bosch D and Keller F (2002) The Cretaceous Ladakh arc of NW Himalaya—slab melting and melt-mantle interaction during fast northward drift of Indian Plate. *Chemical Geology* 182, 139–78.
- Saini HS, Tandon SK, Mujtaba SAI, Pant NC and Khorana RK (2009) Reconstruction of buried channel-floodplain systems of the northwestern Haryana Plains and their relation to the 'Vedic' Saraswati. *Current Science* **97**(11), 1634–43.
- Schärer U, Copeland, P Harrison TM and Searle MP (1990) Age, cooling history, and origin of post-collisional leucogranites in the Karakoram Batholith; a multi-system isotope study. *Journal of Geology* **98**(2), 233–51.
- Singh G, Wasson RJ and Agarwal DP (1990) Vegetational and Seasonal Climatic Changes Since the Last Full Glacial in the Thar Desert Northwestern India. *Review of Palaeobotany and Palynology* 64, 351–58.
- Singh M, Sharma M and Tobschall HJ (2005) Weathering of the Ganga alluvial plain, northern India: implications from fluvial geochemistry of the Gomati River. *Applied Geochemistry* **20**, 1–21, doi: 10.1016/j.apgeochem.2004.07.005.
- **Singhvi AK and Kar A** (1992) *Thar Desert in Rajasthan*. Bangalore: Geological Society of India.
- Singhvi AK, Williams MAJ, Rajaguru SN, Misra VN, Chawla S, Stokes S, Chauhan N, Francis T, Ganjoo RK and Humphreys GS (2010) A 200 ka record of climatic change and dune activity in the Thar Desert, India. *Quaternary Science Reviews* 29(23–24), 3095–105, doi: 10.1016/j.quascire v2010.08.003.
- Srivastava A (2023) Dune Accumulation Chronologies from the Thar Desert, India: A Review. In Sand Dunes of the Northern Hemisphere: Distribution, Formation, Migration and Management (eds Q. Lu, M. K. Gaur and V. R. Squires). CRC Press. 1, doi: 10.1201/9781003125426.
- Stern CR, Kligfield R, Schelling D, Virdi NS, Futa K and Peterman ZE (1989)
  The Bhagirathi leucogranite of High Himalaya (Garhwal, India): age, petrogenesis, and tectonic implications. In *Tectonics of the Western Himalayas* (ed L. L. Malinconico). Boulder, CO: Geological Society of America. Special paper, 232, 33–45.
- Tandon SK and Sinha R (2022) Geology of large river systems. In *Large Rivers*. 7–41, doi: 10.1002/9781119412632.ch2.
- **Taylor SR and McLennan SM** (1995) The geochemical evolution of the continental crust. *Reviews of Geophysics* **33**, 241–65.
- Tripathi JK, Bock B, Rajamani V and Eisenhauer A (2004) Is River Ghaggur, Saraswati? Geochemical constraints. *Current Science* 87(8), 1141–45.

Usman M (2024) Source-to-Sink Sediment Dynamics in Humid and Arid Environments from the Modern Minjiang River, South China and Thar Desert, Pakistan. Università degli Studi di Milano-Bicocca.

- Usman M, Clift PD, Pastore G, Vezzoli G, Andò S, Barbarano M, Vermeesch P and Garzanti E (2024) Climatic influence on sediment distribution and transport in the Thar Desert (Sindh and Cholistan, Pakistan). *Earth-Science Reviews* **249**, 104674, doi: 10.1016/j.earscirev.2024.104674.
- Viers J, Dupré B and Gaillardet J (2009) Chemical composition of suspended sediments in World Rivers: New insights from a new database. Science of The Total Environment 407(2), 853–68, doi: 10.1016/j.scitotenv.2008.09.053.
- Vögeli N, van der Beek P, Huyghe P and Najman Y (2017) Weathering in the Himalaya, an East-West Comparison: indications from major elements and clay mineralogy. *The Journal of Geology* 125, 515–29, doi: 10.1086/ 692652.
- von Eynatten H, Tolosana-Delgado R and Karius V (2012) Sediment generation in modern glacial settings: Grain-size and source-rock control on sediment composition. Sedimentary Geology 280, 80–92, doi: 10.1016/j.se dgeo.2012.03.008.

- von Eynatten H, Tolosana-Delgado R, Karius V, Bachmann K and Caracciolo L (2016) Sediment generation in humid Mediterranean setting: Grain-size and source-rock control on sediment geochemistry and mineralogy (Sila Massif, Calabria). Sedimentary Geology 336, 68–80, doi: 10.1016/j.sedgeo.2015.10.008.
- West AJ, Galy A and Bickle MJ (2005) Tectonic and climatic controls on silicate weathering. *Earth and Planetary Science Letters* 235, 211–28, doi: 10.1016/j.epsl.2005.03.020.
- Whittington A, Foster G, Harris N, Vance D and Ayres M (1999) Lithostratigraphic correlations in the western Himalaya An isotopic approach. *Geology* 27(7), 585–88.
- Zeng N and Yoon J (2009) Expansion of the world's deserts due to vegetationalbedo feedback under global warming. *Geophysical Research Letters* **36**(17), doi: 10.1029/2009GL039699.
- Zhisheng A, Clemens SC, Shen J, Qiang X, Jin Z, Sun Y, Prell WL, Luo J, Wang S, Xu H, Cai Y, Zhou W, Liu X, Liu W, Shi Z, Yan L, Xiao X, Chang H, Wu F, Ai L and Lu F (2011) Glacial-Interglacial Indian Summer Monsoon Dynamics. Science 333(6043), 719–23, doi: 10.1126/science.1203752.